# Lp stability of networked control systems implemented on WirelessHART

Alejandro I. Maass, Dragan Nešić, Romain Postoyan, Peter Dower

# $\mathcal{L}_p$ stability of networked control systems implemented on WirelessHART ⋆

Alejandro I. Maass [a], Dragan Nešić [a], Romain Postoyan [b], Peter M. Dower [a]

[a] *Department of Electrical and Electronic Engineering, The University of Melbourne, Parkville, 3010, Victoria, Australia*

[b] *Université de Lorraine, CNRS, CRAN, F-54000 Nancy, France*

**Abstract**

This paper provides results on input-output $\mathcal{L}_p$ stability of networked control systems (NCSs) implemented over WirelessHART (WH). WH is a communication protocol widely used in process instrumentation. It is mainly characterised by its multi-hop structure, slotted communication cycles, and the possibility to simultaneously transmit over different frequencies. We propose a non-linear hybrid model of WH–NCSs that is able to capture these network functionalities, and that it is more general than existing models in the literature. Particularly, the multi-hop nature of the network is translated into an interesting mathematical structure in our model. We then follow the emulation approach to stabilise the NCS. We first assume that we know a stabilising controller for the plant without the network. We subsequently show that, under reasonable assumptions on the scheduling protocol, stability is preserved when the controller is implemented over the network with sufficiently frequent data transmission. Specifically, we provide bounds on the maximum allowable transmission interval (MATI) under which all protocols that satisfy the property of being *persistently exciting (PE)* lead to $\mathcal{L}_p$ stable WH–NCSs. These bounds exploit the mathematical structure of our WH–NCS model, improving the existing bounds in the literature. Additionally, we explain how to schedule transmissions over the hops to satisfy the PE property. In particular, we show how simultaneous transmissions over different frequency channels can be exploited to further enlarge the MATI bound.

*Key words:* Networked control, WirelessHART, Non-linear systems, $\mathcal{L}_p$ stability.

## 1 Introduction

Networked control systems (NCSs) have received much interest during the last years due to their many practical implications [11, 13]. While the available results are able to capture the essential effects that communication constraints have on the closed-loop system, it remains unclear how these results can be applied to specific physical networks. In this paper, we are motivated to develop results tailored to NCSs implemented over wireless multi-hop networks, which are increasingly used in industry control. Particularly, we study WirelessHART (WH), the first open wireless communication standard for measurement and control in the process industries [1]. According to many international companies, it serves as a compelling alternative for industrial control, as it improves operations, increases productivity, and saves money [1]. WH is a mesh network which utilises field devices in a multi-hop fashion and schedule these via time division multiple access (TDMA).

WH has received a lot of attention in the last decade, both heuristically [4, 8, 10, 21] and analytically [2, 3, 7, 20, 28, 29, 31, 32]. In particular, scheduling in WH is addressed in [20, 28, 29, 31], where several scheduling protocols tailored to different networking requirements can be found. These works focus on the network itself and do not use it in a control loop. Regarding control systems that use a WH network to transmit packets in the control loop, we can find controller-communication co-design in [7, 32]. The authors in [32] developed an LQG framework to study minimum-energy packet forwarding policies for communicating sensor measurements over a WH network. The recent work [7] completes the literature by considering both packet-forwarding and controller co-design. Modelling of WH–NCSs is addressed in [2, 3]. In [3], the authors propose a mathematical frame-

⋆ Corresponding author A.I. Maass. This work was supported by the ARC Discovery Scheme, grant number DP170104099, and by the ANR project COMPACS, ANR-13-BS03-004-02.

*Email addresses:* amaass@student.unimelb.edu.au (Alejandro I. Maass), dnesic@unimelb.edu.au (Dragan Nešić), romain.postoyan@univ-lorraine.fr (Romain Postoyan), pdower@unimelb.edu.au (Peter M. Dower).

work for modelling and analysis of multi-hop networks designed for linear discrete-time systems consisting of multiple control loops closed over a multi-hop wireless communication network. They separate control, topology, routing, and scheduling and propose formal syntax and semantics for the dynamics of the composed system, providing an explicit translation of multi-hop control networks to switched systems. A similar work is [2], in which the formulation, modelling and design of a fixed structure topology for potential application in wireless NCSs is provided. The setup consists of a discrete-time plant, an output feedback discrete-time controller, and intermediate transfer and receiving networks.

The first purpose of this study is to provide a modelling framework that encompasses the models used in [2,3,7,32] by considering a more general class of models that result from a careful study of the WH network. Note that the existing models of WH–NCSs in [2,3,7,32] assume the plant and controller to be discrete-time linear systems. That is, the results are valid only at each transmission instant, but the inter-sample behaviour is lost. This also implies that transmissions in the WH network happen equidistantly. Such assumptions may be hard to satisfy in WH, where extra features need to be considered, e.g. possibly non-linear plant and controller, field-device dynamics, time-varying transmission instants, inter-transmission behaviour given by the continuous plant dynamics, and at-transmission behaviour given by packet transmission. We propose a hybrid model of WH–NCSs that is able to capture all the latter features. More importantly, the multi-hop nature of the network is revealed through our model via an interesting mathematical structure which turns out to be key in our stability analysis.

An important part of the model is the so-called *protocol equation*, which defines how field devices are scheduled in the superframe table of a WH network. It is desired that scheduling protocols satisfy certain properties in order to state our results. A key property is the so-called *persistence of excitation in $T$ ($PE_T$)* [24]. This property was presented in [24] and requires the existence of a fixed number of transmissions $T$ within which all network nodes are visited by the protocol. In WH networks, this translates into every field device being scheduled to transmit within $T$ transmissions. We present a large class of scheduling protocols for which the $PE_T$ property holds. Specifically, we provide three relevant examples that belong to this class and that exploit the flexibility of WH networks, i.e. multiple transmissions over different frequency channels. These results can also be used to design other scheduling policies for field devices in WH.

It was shown in [24] that $PE_T$ protocols lead to $\mathcal{L}_p$ stable NCSs under extra assumptions. However, these results are derived for generic non-linear NCSs in which a packet is immediately received by the controller/plant whenever nodes have access to the network. Therefore, the potential structure of a physical network is not exploited, e.g. multi-hop in WH. We go one step further to [24] and study $\mathcal{L}_p$ stability in WH–NCSs, for which we exploit the mathematical structure of our hybrid model. Specifically, we analyse $\mathcal{L}_p$ stability in the case where the controller is designed by emulation. The main idea of emulation is to first design a controller that stabilises the plant in the absence of the network. Then, the controller is implemented over the network and it is shown that the $\mathcal{L}_p$ stability of the system is preserved, see e.g. [26]. In particular, stability is preserved if the scheduling protocols are persistently exciting, and if data is transmitted at a high enough rate, measured by the *maximum allowable transmission interval* (MATI). We provide two different and easily computable MATI bounds and illustrate in examples that our MATI bounds result to be significantly larger than the ones in [24]. In our preliminary work [16, 17], we presented MATI bounds for disturbance-free WH–NCSs, which resulted to be quite conservative. With this article, we extend our previous results in [16, 17] by considering external disturbances and by providing much tighter MATI bounds.

In brief, the primary contributions of this paper are:

(1) We provide a hybrid model for WH–NCSs that captures both at- and inter-transmission behaviour, time-varying transmission instants, field device dynamics, and non-linear plant and controller, thus generalising the models in [2, 3, 7, 32].
(2) Our model reveals a mathematical structure that comes directly from the features of WH, i.e. multi-hop and buffer dynamics. Previous generic models for non-linear NCSs like [5,18,24,26], although they can be used to analyse our WH–NCS, these do not exploit these features and thus provide more conservative results.
(3) We provide a large class of protocols that satisfy the property of being $PE_T$, which is natural in WH networks. We provide three relevant examples that are implementable in WH and belong to this class.
(4) We provide two different and easily computable MATI bounds that ensure the $\mathcal{L}_p$ stability of our WH–NCS, and that exploit the mathematical structure of our model. We illustrate in examples that our MATI bounds result to be significantly larger than the ones in [24].
(5) We extend our previous results in [16,17] by considering external disturbances and by providing significantly less conservative MATI bounds.

The paper is organized as follows. Notation and preliminaries are given in Section 2. Section 3 describes the WH standard in detail. We present the WH–NCS model in Section 4 and scheduling is analysed in Section 5. $\mathcal{L}_p$ stability results are stated in Section 6. A linear case study is addressed in Section 7. Numerical examples are given in Section 8, whilst Section 9 draws conclusions.

## 2 Preliminaries

### 2.1 Notation

Denote by $\mathbb{R}$ the set of real numbers, $\mathbb{R}^n$ the set of all real vectors with $n$ components, and $\mathbb{R}^{m\times n}$ the set of all real matrices of dimension $m \times n$. Let $\mathbb{R}_{\geq 0} \doteq [0, \infty)$, $\mathbb{Z}_{\geq 0} \doteq \{0, 1, 2, \dots\}$, and $\mathbb{N} \doteq \{1, 2, 3, \dots\}$. Let $\mathcal{A}^n_{\geq 0}$ denote the set of all $n \times n$ matrices with nonnegative entries, and let $\mathbb{R}^n_{\geq 0}$ denote the nonnegative orthant of $\mathbb{R}^n$. A function $\alpha : \mathbb{R}_{\geq 0} \to \mathbb{R}_{\geq 0}$ is of class $\mathcal{K}$ if it is continuous, zero at zero and strictly increasing. It is of class $\mathcal{K}_\infty$ if it is of class $\mathcal{K}$ and unbounded. A function $\beta : \mathbb{R}_{\geq 0} \times \mathbb{R}_{\geq 0} \to \mathbb{R}_{\geq 0}$ is of class $\mathcal{KL}$ if $\beta(\cdot, t)$ is of class $\mathcal{K}$ for each $t \geq 0$, and if $\beta(s, \cdot)$ is continuous, non-increasing and satisfies $\lim_{t\to\infty} \beta(s, t) = 0$ for each $s \geq 0$. Given $t \in \mathbb{R}$ and a piecewise continuous function $f : \mathbb{R} \to \mathbb{R}^n$, we use the notation $f(t^+) \doteq \lim_{s\to t, s>t} f(s)$. For simplicity, we use $(x, y) \doteq [x^T \;\; y^T]^T \in \mathbb{R}^{n+m}$, for any $x \in \mathbb{R}^n$ and $y \in \mathbb{R}^m$. For a vector $x = (x_1, \dots, x_n) \in \mathbb{R}^n$, $\|x\|_p \doteq (\sum_{i=1}^n |x_i|^p)^{1/p}$, for all $p \in [1, \infty)$, and $\|x\|_\infty \doteq \max_i |x_i|$. To ease notation, we use $|x|$ to denote $\|x\|_2$. The same notation is used to denote the induced 2-norm of a matrix. For an $m \times n$ matrix $A$, the induced matrix 1-norm is given by $\|A\|_1 \doteq \max_{1\leq j\leq n} \sum_{i=1}^m |a_{ij}|$. $I_n$ stands for the $n \times n$ identity matrix. We also use $\mathbf{I}_n^N \doteq [I_n \;\cdots\; I_n]^N$ to denote the matrix $[I_n \;\cdots\; I_n] \in \mathbb{R}^{n\times Nn}$. We will often consider vectors of the form $\bar{x}$, where $x \in \mathbb{R}^n$ and $\bar{x} \doteq (|x_1|, \dots, |x_n|)^T$. For a function $f : \mathbb{R} \to \mathbb{R}^n$, we define $\bar{f} : t \to \overline{f(t)}$. Let $Df(t)$ denote the left-handed derivative of $f : \mathbb{R} \to \mathbb{R}^n$, if it exists, i.e. $Df(t) \doteq \lim_{h\to 0, h<0} \frac{f(t+h)-f(t)}{h}$. We define $\mathbb{1}_S$ as the function $\mathbb{1}_S : \mathbb{N} \to \{0, 1\}$ such that $\mathbb{1}_S(i) = 1$ if $i \in S$, and $\mathbb{1}_S(i) = 0$ if $i \notin S$. Let $f : \mathbb{R} \to \mathbb{R}^n$ be a (Lebesgue) measurable function and define

$$\|f\|_{\mathcal{L}_p} \doteq \left( \int_{\mathbb{R}} \|f(s)\|^p \, ds \right)^{1/p}, \tag{1}$$

for $p \in \mathbb{N}$, $\|f\|_{\mathcal{L}_\infty} \doteq \operatorname{ess\,sup}_{t\in\mathbb{R}} \|f(t)\|$, and $\|f\|_{\mathcal{L}_\infty[a,b]} \doteq \operatorname{ess\,sup}_{t\in[a,b]} \|f(t)\|$. Note that $\|\cdot\|$ in (1), for any $p \in [1, \infty]$, can be any $p$-norm on $\mathbb{R}^n$ [14]. We use the Euclidean norm $\|\cdot\| \doteq |\cdot|$ as default throughout the paper. However, at the end of Section 6 we use the $p$-norm on $\mathbb{R}^n$, i.e. $\|\cdot\| \doteq \|\cdot\|_p$, which will become clear from the context. Let $f : \mathbb{R} \to \mathbb{R}^n$ and let $[a, b] \subset \mathbb{R}$, we use the notation $\|f\|_{\mathcal{L}_p[a,b]} \doteq \left( \int_{[a,b]} \|f(s)\|^p \, ds \right)^{1/p}$, to denote the $\mathcal{L}_p$ norm of $f$ when restricted to the interval $[a, b]$. For $T \in \mathbb{N}$, we define a collection of sequences of $n\times n$ matrices $\mathfrak{S}_n(T)$, such that, for all $s \in \mathbb{N}$, $\{A_i\}_{i\in\mathbb{N}} \in \mathfrak{S}_n(T)$ if and only if $\prod_{i=s}^{s+T-1} A_i = 0$. Let $x = (x_1, \dots, x_n), y = (y_1, \dots, y_n) \in \mathbb{R}^n$. A partial order $\preceq$ is given by $x \preceq y \iff x_i \leq y_i$, for all $i \in \{1, \dots, n\}$. We define an analogous partial order on elements of $\mathcal{A}^n_{\geq 0}$ in the natural way, i.e. $A \preceq B \iff B - A \in \mathcal{A}^n_{\geq 0}$.

### 2.2 Underlying stability theory

Consider the jump-flow (hybrid system) model $\Sigma$,

$$\dot{z} = f(t, z, w), \; t \in [t_i, t_{i+1}], \tag{2a}$$
$$z(t_i^+) = h(i, z(t_i)), \tag{2b}$$
$$y = H(t, z), \tag{2c}$$

where $z \in \mathbb{R}^{n_z}$ is the state, $w \in \mathbb{R}^{n_w}$ is an exogenous perturbation, $y \in \mathbb{R}^{n_y}$ is a prescribed output, $n_z, n_w, n_y \in \mathbb{N}$, and $\{t_i\}_{i=0}^\infty$ is a sequence of increasing time instants such that, for some $\tau \in \mathbb{R}$ and $\varepsilon > 0$, $\varepsilon < t_{i+1} - t_i < \tau < \infty$ for all $i \in \mathbb{N}$. Suppose $\Sigma$ is initialised at $(t_0, z_0)$ with input $w$. We assume enough regularity on $f$ and $h$ to guarantee existence of the solution $z(\cdot) = z(\cdot, t_0, z_0, w)$ on the interval of interest, see [18].

We now define the stability notions used throughout this paper.

**Definition 1** *Let $p \in \mathbb{N} \cup \{+\infty\}$ and $\gamma \geq 0$ be given. We say that $\Sigma$ is $\mathcal{L}_p$ stable from $w$ to $y$ with gain $\gamma$ if there exists $K \geq 0$ such that $\|y\|_{\mathcal{L}_p[t_o,t]} \leq K|z_0| + \gamma\|w\|_{\mathcal{L}_p[t_0,t]}$, for all $t \geq t_0$, $w \in \mathcal{L}_p[t_0, t]$ and $z_0 \in \mathbb{R}^{n_z}$.* ■

**Definition 2** *Let $p, q \in \mathbb{N} \cup \{+\infty\}$ and $\gamma \geq 0$ be given. The state $z$ of $\Sigma$ is said to be $\mathcal{L}_p$ to $\mathcal{L}_q$ detectable from $(y, w)$ with gain $\gamma$ if there exists $K \geq 0$ such that $\|z\|_{\mathcal{L}_q[t_0,t]} \leq K|z_0| + \gamma\|y\|_{\mathcal{L}_p[t_0,t]} + \gamma\|w\|_{\mathcal{L}_p[t_0,t]}$, for all $t \geq t_0$, $y \in \mathcal{L}_p[t_0, t]$, $w \in \mathcal{L}_p[t_0, t]$ and $z_0 \in \mathbb{R}^{n_z}$.* ■

Consider the feedback interconnection of two systems $\Sigma_1$ and $\Sigma_2$, each one of the same form as $\Sigma$ in (2), that is

$$\Sigma_1 \begin{cases} \dot{x}_1 = f_1(t, x_1, x_2, w), \; t \in [t_i, t_{i+1}], \\ x_1(t_i^+) = h_1(i, x_1(t_i)), \\ y_1 = H_1(t, x_1, y_2, w), \end{cases} \tag{3}$$

$$\Sigma_2 \begin{cases} \dot{x}_2 = f_2(t, x_1, x_2, w), \; t \in [t_i, t_{i+1}], \\ x_2(t_i^+) = h_2(i, x_2(t_i)), \\ y_2 = H_2(t, y_1, x_2, w). \end{cases} \tag{4}$$

This interconnection admits a small-gain theorem presented in [18, Section II-B], which will later be used to prove our main stability result.

**Theorem 1** *Suppose that $p, q \in \mathbb{N} \cup \{+\infty\}$, and the following hold:*

*(1) System (3) is $\mathcal{L}_p$ stable from $(y_2, w)$ to $y_1$ with gain $\gamma_1$;*
*(2) $x_1$ in (3) is $\mathcal{L}_p$ to $\mathcal{L}_q$ detectable from $(y_1, w)$;*
*(3) (4) is $\mathcal{L}_p$ stable from $(y_1, w)$ to $y_2$ with gain $\gamma_2$;*
*(4) $x_2$ in (4) is $\mathcal{L}_p$ to $\mathcal{L}_q$ detectable from $(y_2, w)$;*
*(5) The small-gain condition $\gamma_1\gamma_2 < 1$ holds.*

*Then, (3)-(4) is $\mathcal{L}_p$ stable from $w$ to $(x_1, x_2)$.* ■

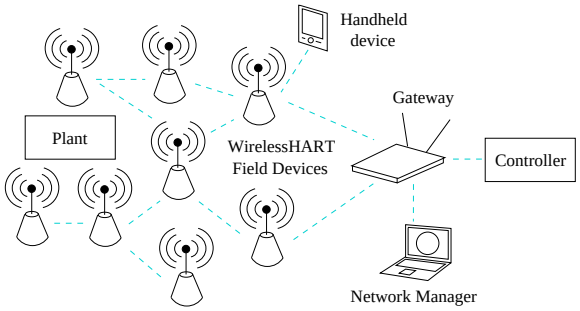


Fig. 1. WirelessHART architecture.

We use the standard notion of uniform global exponential stability (UGES) for system (3)-(4) in the absence of exogenous perturbations.

**Definition 3** *Consider system* $\Sigma$ *and suppose that* $w \doteq 0$. *We say that the origin of* $\Sigma$ *is uniformly globally exponentially stable if there exist* $K, L \geq 0$ *such that, for every* $z_0 \in \mathbb{R}^{n_z}$, $|z(t, t_0, z_0)| \leq K \exp(-L(t - t_0))|z_0|$ *for all* $t \geq t_0$. ■

The following sufficient condition is used to ensure UGES of (3)-(4) in the absence of $w$ [24].

**Theorem 2** *Suppose that systems* (3) *and* (4) *satisfy all hypotheses of Theorem 1. If there exist* $L_1, L_2, L_3, L_4 \geq 0$ *such that* $|f_1(t, x_1, x_2, 0)| \leq L_1(|x_1| + |x_2|)$, $|f_2(t, x_1, x_2, 0)| \leq L_2(|x_1| + |x_2|)$, $|h_1(i, x_1)| \leq L_3|x_1|$, $|h_2(i, x_2)| \leq L_4|x_2|$, *for all* $x_1 \in \mathbb{R}^{n_{x_1}}$, $x_2 \in \mathbb{R}^{n_{x_2}}$, $n_{x_1}, n_{x_2} \in \mathbb{N}$, *all* $t \geq t_0$ *and all* $i \in \mathbb{N}$. *Then,* (3)-(4) *with* $w \doteq 0$ *is UGES.* ■

## 3 WirelessHART Network

In the following, a description of WH and the adopted assumptions are provided.

### *3.1 Communication features*

The general architecture of WH is shown in Fig. 1. It consists of an interconnection of basic components including field devices (sensor, actuators and routers), handheld devices, gateways, and a network manager. WH is based on the IEEE 802.15.4-2006 physical layer and operates in the 2.4 GHz ISM radio band with a maximum data rate of 250 kbps over 15 frequency division multiplexed channels. In the data link layer, WH defines a slotted TDMA technology. That is, each frequency channel is subdivided into timeslots in which an assigned field device is allowed to transmit. WH networks also support multiple access timeslots, where multiple devices can share a specific channel. In this case, WH uses *carrier sense multiple access with collision avoidance* (CSMA/CA) mechanisms to avoid collisions. We restrict our attention to TDMA in this paper. We study WH–NCSs under CSMA in our recent work [15].

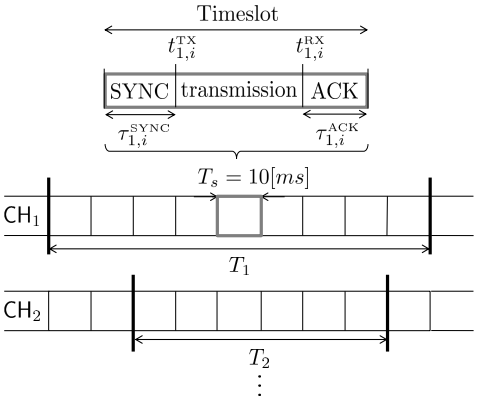


Fig. 2. WirelessHART superframe table.

### *3.2 TDMA superframe structure*

All communications in a WH network are defined with respect to a *superframe*. For each $l$-th channel, $l = 1, \ldots, 15$, a superframe is an a priori fixed period of time $T_l > 0$, contiguous in real time with other superframes within each channel, that is divided into a sequence of timeslots as depicted in Fig. 2. Field devices are scheduled to transmit in the superframe, and each one of the 15 channels may have a different superframe depending on the chosen scheduling protocol. The set of superframes across frequency channels is called a *superframe table*. Each timeslot is strictly $T_s = 10[ms]$ in duration. Within this timeslot, a complete single data packet and its corresponding acknowledgement are transmitted between two field devices. The transmission delay required for the delivery of a packet from a transmitting device to a receiving device, in each $l$-th channel and $i$-th timeslot, is denoted by $t_{l,i}^{\mathrm{RX}} - t_{l,i}^{\mathrm{TX}}$ and it depends on the packet size. For each channel $l$-th channel and at the end of every $i$-th timeslot, the time it takes to acknowledge such a packet is denoted by $\tau_{l,i}^{\mathrm{ACK}}$. For effective TDMA communications, all devices need to be synchronized. This is ensured, at the beginning of each $i$-th timeslot on the $l$-th channel, by the amount $\tau_{l,i}^{\mathrm{SYNC}}$. For simplicity, the following additional assumption is adopted.

**Assumption 4** *The following holds.*

*(a) Transmissions across all channels are synchronized, i.e.* $\tau_i^{SYNC} \doteq \tau_{l,i}^{SYNC} = \tau_{k,i}^{SYNC}$ *for all* $l, k \in \{1, \ldots, 15\}$. *We define* $\varepsilon \doteq \inf_{i \in \mathbb{N}} \tau_i^{SYNC}$ *and assume that* $\varepsilon > 0$.

*(b) Acknowledgement time is negligible in each timeslot, i.e.* $\tau_{l,i}^{ACK} = 0$ *for all* $l \in \{1, \ldots, 15\}$ *and* $i \in \mathbb{N}$.

*(c) Packets are transmitted instantaneously in every timeslot, i.e.* $t_i \doteq t_{l,i}^{TX} = t_{l,i}^{RX}$ *for all* $l \in \{1, \ldots, 15\}$ *and* $i \in \mathbb{N}$. *We refer to* $t_i$ *as transmission instant.*

*(d) One successful transmission between devices occurs within each timeslot, per channel.* ■

Item (a) is adopted to avoid accounting for clock drift. This assumption is reasonable under the strict synchronization procedure in WH [1]. However, this assumption can be relaxed, and the analytical tools we present in this paper can be used to deal with such scenario. Notation in that case becomes cumbersome and we thus adopt Assumption 4(a) for clarity. In Section 8, we present a simulation in which the WH network is subject to clock drift, and we illustrate that our results still work under this constraint. Items (b) and (c) are reasonable in the context of WH in practice. Note that each timeslot is strictly 10[ms], and the WH specification allocates 832[$\mu$s] for the whole ACK packet. The timeslot length is about 12 times the ACK packet, hence why neglecting it is appropriate. With respect to item (c), please note that the maximum packet length in WH is 127 bytes [6]. We allude to papers like [8, 21], in which the authors have implemented the NCS over a real WH network and measured packet transmission delays, among other values. In these experiments, we can see that the transmission delay ranges from 0.919[ms] to 1[ms]. The timeslot length is then about 10 times the transmission delay, hence why we believe it is appropriate to neglect it. We adopt item (d) so as to restrict attention to the effects of the transmission instants $t_i$ in the modelling. Packet drops are outside the scope of this paper, but are analysed in our recent paper [15] with an analogue stochastic framework.

**Remark 5** *The transmission instants $t_i$ need not be equally spaced between each other depending on synchronization time $\tau_i^{SYNC}$. This models the fact that real-life networks in general have time-varying transmission instants and not necessarily equidistant as often modelled, see [2, 3, 7, 32].* ■

We will parametrize our model with the so-called *maximal allowable transmission interval* (MATI) [26], which we denote as $\tau > 0$. It is a measure of how fast the network needs to transmit in order to preserve stability of the NCS. The next corollary comes from Assumption 4.

**Corollary 1** *If Assumption 4 holds, the transmission instants $t_i$ in the WH network, satisfy $\varepsilon \leq t_{i+1} - t_i \leq \tau \leq 2T_s - \varepsilon$ for all $i \in \mathbb{N}$.* ■

Corollary 1 states that a packet must be transmitted at most in $\tau$ seconds, which cannot be larger than $2T_s - \varepsilon$.

## 4 Model of a WH–NCS

In this section we provide the hybrid modelling framework for WH–NCSs. Consider Fig. 3, where the plant is modelled as a general non-linear system via

$$\dot{x}_p = f_p(x_p, \hat{u}, w), \quad y = g_p(x_p), \tag{5}$$

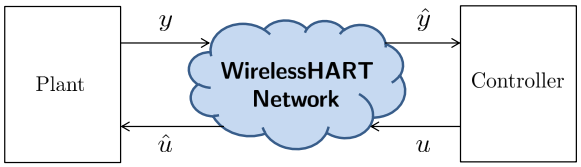


Fig. 3. Block diagram of a NCS over WirelessHART.

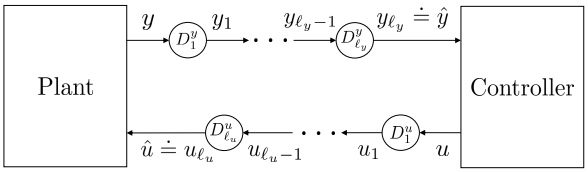


Fig. 4. NCS closed over a WH network with $\ell_y$ field devices in the $y$-path and $\ell_u$ field devices in the $u$-path.

where $x_p \in \mathbb{R}^{n_p}$ is the state, $\hat{u} \in \mathbb{R}^{n_u}$ is the control signal received by the plant, $y \in \mathbb{R}^{n_y}$ is the plant output, $w \in \mathbb{R}^{n_w}$ is an exogenous perturbation which is assumed to belong to $\mathcal{L}_p$, i.e. its $\mathcal{L}_p$ norm is finite for given $p \in [1, \infty]$, and $n_p, n_u, n_y, n_w \in \mathbb{N}$. The controller is also modelled as a non-linear system given by

$$\dot{x}_c = f_c(x_c, \hat{y}, w), \quad u = g_c(x_c), \tag{6}$$

where $x_c \in \mathbb{R}^{n_c}$ is the state of the controller, $\hat{y} \in \mathbb{R}^{n_y}$ is the plant output received by the controller, $u \in \mathbb{R}^{n_u}$ is the control signal, and $n_c \in \mathbb{N}$. The functions $f_p, f_c$ are assumed to be continuous and $g_p, g_c$ are assumed to be continuously differentiable.

We now model the WH network based on the description and assumptions provided in Section 3. Particularly, we model the WH network as in Fig. 4, i.e. we consider $\ell_y \in \mathbb{Z}_{\geq 0}$ field devices interconnected in the plant-to-controller path ($y$-path), and $\ell_u \in \mathbb{Z}_{\geq 0}$ in the controller-to-plant path ($u$-path). We label field devices as $D^y_\alpha$ and $D^u_\beta$, where $\alpha = 1, \ldots, \ell_y$ and $\beta = 1, \ldots, \ell_u$. For each field device, its inputs and outputs are depicted in Fig. 4. The signal that reaches the controller (resp. plant) in Fig. 4, i.e. $y_{\ell_y}$ (resp. $u_{\ell_u}$), is denoted as $\hat{y}$ (resp. $\hat{u}$) to be consistent with Fig. 3 and existent NCS literature. Each field device acts as a router for data from/to neighbouring field devices and we model them as buffers. We introduce buffer state variables $b^y_\alpha$ and $b^u_\beta$ for field devices in the $y$-path and $u$-path, respectively. We now explain the reception and transmission behaviour of field devices, and we present the corresponding equations. We treat field devices as zero-order-hold devices, in which their buffer value and output are held between transmissions.

**Reception:** Suppose a field device $D^y_\alpha$ receives a packet at time instant $t_i$. Then, $D^y_\alpha$ updates the content of its buffer via its input. During this process, the output of $D^y_\alpha$ remains unchanged. We write this as follows,

$$\dot{y}_\alpha(t) = 0, \quad \dot{b}^y_\alpha(t) = 0, \quad t \in [t_i, t_{i+1}], \tag{7a}$$
$$b^y_\alpha(t_i^+) = y_{\alpha-1}(t_i^+), \quad y_\alpha(t_i^+) = y_\alpha(t_i). \tag{7b}$$

for all $\alpha = 1, \dots, \ell_y$. Note that $y_0 \doteq y$ for $\alpha = 1$, i.e. device one samples the value of the plant output.

**Transmission:** Suppose a field device $D^y_\alpha$ is scheduled to transmit at time instant $t_i$. Here, $D^y_\alpha$ sends the content of its buffer through its output, and keeps it until a new packet is received. This can be written as follows,

$$\dot{y}_\alpha(t) = 0, \quad \dot{b}^y_\alpha(t) = 0, \quad t \in [t_i, t_{i+1}], \tag{8a}$$
$$y_\alpha(t_i^+) = b^y_\alpha(t_i), \quad b^y_\alpha(t_i^+) = b^y_\alpha(t_i), \tag{8b}$$

for all $\alpha = 1, \dots, \ell_y$.

Motivated by (8)-(7), we introduce the network-induced error $\zeta \in \mathbb{R}^{n_\zeta}$, with $n_\zeta \doteq n_{\zeta^y} + n_{\zeta^u}$, $n_{\zeta^y} \doteq 2\ell_y n_y$, and $n_{\zeta^u} \doteq 2\ell_u n_u$. We define it as $\zeta \doteq (\zeta^y, \zeta^u)$, where $\zeta^y \in \mathbb{R}^{n_{\zeta^y}}$ and $\zeta^u \in \mathbb{R}^{n_{\zeta^u}}$ are the corresponding errors of the $y$-path and $u$-path, respectively, and are given by

$$\begin{aligned}\zeta^y &= \big(\zeta^y_1, \zeta^y_2, \dots, \zeta^y_{\ell_y}, \zeta^y_{\ell_y+1}, \zeta^y_{\ell_y+2}, \dots, \zeta^y_{2\ell_y}\big) \\ &\doteq \big(b^y_1 - y, b^y_2 - y_1, \dots, b^y_{\ell_y} - y_{\ell_y - 1}, \\ &\qquad y_1 - b^y_1, y_2 - b^y_2, \dots, y_{\ell_y} - b^y_{\ell_y}\big), \end{aligned} \tag{9a}$$
$$\begin{aligned}\zeta^u &= \big(\zeta^u_1, \zeta^u_2, \dots, \zeta^u_{\ell_u}, \zeta^u_{\ell_u+1}, \zeta^u_{\ell_u+2}, \dots, \zeta^u_{2\ell_u}\big) \\ &\doteq \big(b^u_1 - u, b^u_2 - u_1, \dots, b^u_{\ell_u} - u_{\ell_u - 1}, \\ &\qquad u_1 - b^u_1, u_2 - b^u_2, \dots, u_{\ell_u} - b^u_{\ell_u}\big). \end{aligned} \tag{9b}$$

The first $\ell_\star$ components of $\zeta^\star$, $\star \in \{y, u\}$, are related to the buffer update during reception, and we call these *reception errors*. The remaining $\ell_\star$ components of $\zeta^\star$ are related to the transmission of such buffer value through their output, and we call them *transmission errors*. In particular, we reset to zero these errors to model reception and transmission. This is a major difference with previous models of non-linear NCSs like [5, 18, 26], in which the network-induced error is given by $e \doteq (\hat{y} - y, \hat{u} - u)$ (i.e. no specific network is considered, and the possible buffer dynamics are ignored). Specifically, whenever there is a transmission, this error models it as the plant (resp. controller) receiving the sensor (resp. actuator) packet immediately. In WH networks, this is not always the case, as the packet needs to travel along different field devices before it reaches its destination, generating an intrinsic delay. Therefore, dynamics of field devices have to be taken into account, together with a proper definition of the network-induced error, as in (9).

Now that all components of Fig. 4 have been modelled, we are in a position to present the model for a WH–NCS. Define the augmented state $x \doteq (x_p, x_c)$, where $x \in \mathbb{R}^{n_x}$. By using (5), (6), (7), (8), and (9), we present a hybrid model for the block diagram in Fig. 4,

$$\dot{x}(t) = f(x(t), \zeta(t), w), \quad t \in [t_i, t_{i+1}], \tag{10a}$$
$$\dot{\zeta}(t) = g(x(t), \zeta(t), w), \quad t \in [t_i, t_{i+1}], \tag{10b}$$
$$x(t_i^+) = x(t_i), \tag{10c}$$
$$\zeta(t_i^+) = \mathcal{H}(i)\zeta(t_i), \tag{10d}$$

where $i \in \mathbb{N}$, $f : \mathbb{R}^{n_x} \times \mathbb{R}^{n_\zeta} \times \mathbb{R}^{n_w} \to \mathbb{R}^{n_x}$ and $g : \mathbb{R}^{n_x} \times \mathbb{R}^{n_\zeta} \times \mathbb{R}^{n_w} \to \mathbb{R}^{n_\zeta}$ are defined as

$$\begin{aligned} f(x, \zeta, w) \doteq \Big(&f_p(x_p, \mathbf{I}^{2\ell_u}_{n_u} \cdot \zeta^u + g_c(x_c), w), \\ &f_c(x_c, \mathbf{I}^{2\ell_y}_{n_y} \cdot \zeta^y + g_p(x_p), w)\Big), \end{aligned} \tag{11}$$

$$\begin{aligned} g(x, \zeta, w) \doteq \\ \Big(&-\frac{\partial g_p}{\partial x_p} f_p(x_p, \mathbf{I}^{2\ell_u}_{n_u} \cdot \zeta^u + g_c(x_c), w), 0, \dots, 0, \\ &-\frac{\partial g_c}{\partial x_c} f_c(x_c, \mathbf{I}^{2\ell_y}_{n_y} \cdot \zeta^y + g_p(x_p), w), 0, \dots, 0\Big), \end{aligned} \tag{12}$$

and where $\mathcal{H}(i)$ is a time-varying matrix that decides when field devices are scheduled to transmit. In particular, this matrix will zero components of $\zeta(t_i^+)$ according to how devices are scheduled in the superframe table. We refer to $\zeta(t_i^+) = \mathcal{H}(i)\zeta(t_i)$ as the *protocol equation*, which is properly studied in Section 5.

## 5 Scheduling protocols

In this section, we first explain how scheduling protocols can be translated into the form (10d). We then define a large class of protocols for which its protocol equation satisfies the property of being *persistently exciting*. This property will be key to ensuring $\mathcal{L}_p$ stability of (10). To finalise, we give three relevant protocols which belong to this class and that exploit the flexibility of the network.

### 5.1 Constructing the protocol equation

In order to have proper TDMA communications in WH, the construction of the superframe table has to satisfy the following requirements from the WH standard [1]:

- *(i)* Only one transmission per frequency channel per timeslot may be scheduled between field devices.
- *(ii)* A field device cannot transmit and receive at the same time.
- *(iii)* All 15 available frequency channels may be used to schedule transmissions.
- *(iv)* Superframes along frequency channels may have different periods.

To construct the protocol equation (10d) associated to the superframe table, we need to follow the above requirements together with the dynamics (8)-(7) of the field devices. We proceed to illustrate this process by a simple example. Let us consider Table 1, where devices are scheduled in a WH network with $\ell_y = 2$, $\ell_u = 0$, using a single frequency channel, denoted by $\mathsf{CH}_1$. Note that $\zeta = \zeta^y$ given that $\ell_u = 0$. Based on (8), (7) and Table 1, we now show how the network error $\zeta^y$ behaves at $t_i^+$, for $i \in \mathbb{N}$. At time instant $t_1$, $D^y_1$ updates its buffer value with the plant output, and the rest of outputs and

Table 1
Example of a superframe table constructed under the requirements of the WH standard.

| | $t_1$ | $t_2$ | $t_3$ |
|---|---|---|---|
| $\mathsf{CH}_1$ | $P \to D_1^y$ | $D_1^y \to D_2^y$ | $D_2^y \to C$ |

buffer values remain constant. Hence, the reception error associated with $D_1^y$ gets reset to zero, that is

$$\zeta^y(t_1^+) = \begin{bmatrix} b_1^y(t_1^+) - y(t_1^+) \\ b_2^y(t_1^+) - y_1(t_1^+) \\ y_1(t_1^+) - b_1^y(t_1^+) \\ y_2(t_1^+) - b_2^y(t_1^+) \end{bmatrix} = \begin{bmatrix} 0 \\ \zeta_2^y(t_1) \\ y_1(t_1) - y(t_1) \\ \zeta_4^y(t_1) \end{bmatrix} = \begin{bmatrix} 0 & 0 & 0 & 0 \\ 0 & I_{n_y} & 0 & 0 \\ I_{n_y} & 0 & I_{n_y} & 0 \\ 0 & 0 & 0 & I_{n_y} \end{bmatrix} \zeta^y(t_1).$$

At time instant $t_2$, $D_1^y$ transmits its buffer value towards $D_2^y$. After this transmission the buffer value $b_1^y$ remains unchanged, and $b_2^y$ gets updated. Hence, the transmission error associated with $D_1^y$ gets reset to zero, and the reception error associated with $D_2^y$ gets reset to zero,

$$\zeta^y(t_2^+) = \begin{bmatrix} \zeta_1^y(t_2) \\ 0 \\ 0 \\ y_2(t_2) - b_1(t_2) \end{bmatrix} = \begin{bmatrix} I_{n_y} & 0 & 0 & 0 \\ 0 & 0 & 0 & 0 \\ 0 & 0 & 0 & 0 \\ 0 & I_{n_y} & I_{n_y} & I_{n_y} \end{bmatrix} \zeta^y(t_2).$$

Finally, at time instant $t_3$, $D_2^y$ transmits its buffer value to the controller, thus the transmission error associated with $D_2^y$ gets reset to zero. That is,

$$\zeta^y(t_3^+) = \begin{bmatrix} b_1^y(t_3^+) - y(t_3^+) \\ b_2^y(t_3^+) - y_1(t_3^+) \\ y_1(t_3^+) - b_1^y(t_3^+) \\ y_2(t_3^+) - b_2^y(t_3^+) \end{bmatrix} = \begin{bmatrix} I_{n_y} & 0 & 0 & 0 \\ 0 & I_{n_y} & 0 & 0 \\ 0 & 0 & I_{n_y} & 0 \\ 0 & 0 & 0 & 0 \end{bmatrix} \zeta^y(t_3).$$

Consequently, the above generates the protocol equation $\zeta^y(t_i^+) = \mathcal{H}^y(i)\zeta^y(t_i)$, $i \in \mathbb{N}$, where $\mathcal{H}^y(i)$ is a time-varying matrix of the form

$$\mathcal{H}^y(i) = \begin{bmatrix} \Delta^y(i) & 0 \\ I - \Delta^y(i) & \Gamma^y(i) \end{bmatrix},$$

where $\Delta^y(i) = \operatorname{diag}\left\{\delta_1^y(i)I_{n_y}, \delta_2^y(i)I_{n_y}\right\}$, and

$$\Gamma^y(i) = \begin{bmatrix} \gamma_1^y(i)I_{n_y} & 0 \\ (1-\gamma_1^y(i))I_{n_y} & \gamma_2^y(i)I_{n_y} \end{bmatrix},$$

with $\delta_\alpha^y(i) = 0$ when $i = \alpha + 3\sigma$ and $\delta_\alpha^y(i) = 1$ otherwise, and $\gamma_\alpha^y(i) = 0$ when $i = \alpha + 1 + 3\sigma$ and $\gamma_\alpha^y(i) = 1$ otherwise, for $\alpha = 1, 2$ and $\sigma \in \mathbb{Z}_{\geq 0}$. Note that the superframe table is periodic, thus the term $3\sigma$ in the above equations. This process can be followed to construct the protocol equation from any superframe table.

In the general case, $\mathcal{H}(i) \doteq \operatorname{diag}\{\mathcal{H}^y(i), \mathcal{H}^u(i)\}$, where

$$\mathcal{H}^\star(i) \doteq \begin{bmatrix} \Delta^\star(i) & 0 \\ I - \Delta^\star(i) & \Gamma^\star(i) \end{bmatrix}, \tag{13}$$

$$\Delta^\star(i) \doteq \operatorname{diag}\left\{\delta_1^\star(i)I_{n_y}, \ldots, \delta_{\ell_\star}^\star(i)I_{n_y}\right\},$$

$$\Gamma^\star(i) \doteq \begin{bmatrix} \gamma_1^\star(i)I_{n_y} & & \\ (1-\gamma_1^\star(i))I_{n_y} & \gamma_2^\star(i)I_{n_y} & \\ & \ddots & \ddots \\ & & (1-\gamma_{\ell_\star-1}^\star(i))I_{n_y} \ \gamma_{\ell_\star}^\star(i)I_{n_y} \end{bmatrix},$$

with $\star \in \{y, u\}$, and $\gamma_\alpha^y(i), \gamma_\beta^u(i), \delta_\alpha^y(i), \delta_\beta^u(i) \in \{0, 1\}$, $\alpha = 1, \ldots, \ell_y, \beta = 1, \ldots, \ell_u$, which are defined differently according to the constructed superframe table. Therefore, given a superframe table, we can construct the protocol equation as done for the example above, and the resulting $\mathcal{H}(i)$ matrix will have the form in (13), with specific definitions of $\gamma_\alpha^y(i), \gamma_\beta^u(i), \delta_\alpha^y(i), \delta_\beta^u(i)$ depending on the chosen table. Later in this section, we provide relevant scheduling protocols that arise in WH networks, for which we give these definitions.

### *5.2 A class of persistently exciting protocols*

We would like to implement scheduling protocols that satisfy the property of being persistently exciting. In this section, we provide a large class of TDMA scheduling protocols that satisfy this property.

**Definition 6** *The protocol* (10d) *is said to be persistently exciting in $T$ ($PE_T$) if there exists $T \in \mathbb{N}$ such that*

$$\prod_{k=i}^{i+T-1} \mathcal{H}(k) = 0, \tag{14}$$

*for every $i \in \mathbb{N}$.* ■

Recall that transmissions are modelled by resetting to zero components of $\zeta(t_i^+)$. Then, we can interpret $PE_T$ protocols in WH as protocols that regularly schedule to transmit every field device within a fixed period of time. Motivated by this, we state the following assumption that will allow us to define the class of $PE_T$ protocols.

**Assumption 7** *Every field device $D_\alpha^y, D_\beta^u$, $\alpha = 1, \ldots, \ell_y, \beta = 1, \ldots, \ell_u$, needs to be scheduled to transmit within a fixed period of time.* ■

Assumption 7 is naturally satisfied by many network technologies such as Ethernet, IEEE 802.11, and IEEE 802.15.4 standard [24], including WirelessHART (WH) networks as we illustrate in Section 5.3. The reason behind it is that Assumption 7 only requires that every field device in the path transmits within a fixed period of time. This is not hard to satisfy as the schedule is designed by the network manager. Additionally, protocols

that have been designed optimally w.r.t. a certain criteria also satisfy Assumption 7, see. e.g. [29,30].

The next lemma states that, if a scheduling protocol satisfies Assumption 7, then such protocol is $PE_T$. The proof is provided in the appendix.

**Lemma 8** *Consider the WH–NCS* (10) *and suppose Assumption 7 holds. Then, the corresponding protocol equation* (10d) *satisfies* (14) *for some* $T \in \mathbb{N}$. ■

We are now in a position to define a class of scheduling protocols that can be implemented in WH and that satisfy the $PE_T$ property.

**Definition 9 (Class of WH-$PE_T$ protocols)** *This class contains all scheduling protocols that satisfy Assumption 7, and thus satisfy the property of being* $PE_T$ *according to Lemma 8.* ■

Constructing scheduling protocols that belong to this class is important. In fact, in Section 6 we show that $PE_T$ protocols lead to $\mathcal{L}_p$ stable WH–NCSs. Therefore, Assumption 7 can be used to design different types of scheduling policies. We now present three relevant examples that belong to the class of WH-$PE_T$ protocols in Definition 6. These are important to illustrate how the flexibility offered by the WH network can be exploited (multiple frequency channels).

### *5.3 Examples of $PE_T$ scheduling protocols*

#### *5.3.1 Simple Round Robin (S-RR)*

This protocol schedules the field devices in a round-robin manner [18], i.e. in a predetermined and cyclic manner. A single frequency channel is used and the field devices communicate one after the other. In particular, we adopt the superframe table shown in Table 2.

Table 2
Superframe table for the S-RR protocol.

| | $t_1$ | $\cdots$ | $t_{\ell_y+1}$ | $t_{\ell_y+2}$ | $\cdots$ | $t_{\ell_y+\ell_u+2}$ |
|---|---|---|---|---|---|---|
| $\mathsf{CH}_1$ | $P \to D_1^y$ | $\cdots$ | $D_{\ell_y}^y \to C$ | $C \to D_1^u$ | $\cdots$ | $D_{\ell_u}^u \to P$ |

For this scheduling protocol, and enlightened by Table 2 and the constructive procedure of Section 5.1, it is possible to show that, $\delta_\alpha^y(i) \doteq 1 - \mathbb{1}_{\mathcal{S}_\alpha^y}(i)$, $\delta_\beta^u(i) \doteq 1 - \mathbb{1}_{\mathcal{S}_\beta^u}(i)$, $\gamma_\alpha^y(i) \doteq 1 - \mathbb{1}_{\bar{\mathcal{S}}_\alpha^y}(i)$, and $\gamma_\beta^u(i) \doteq 1 - \mathbb{1}_{\bar{\mathcal{S}}_\beta^u}(i)$, where

$$\mathcal{S}_\alpha^y \doteq \{i \in \mathbb{N} : i = \alpha + (\ell_y + \ell_u + 2)\sigma, \sigma \in \mathbb{Z}_{\geq 0}\},$$
$$\mathcal{S}_\beta^y \doteq \{i \in \mathbb{N} : i = \beta + \ell_y + 1 + (\ell_y + \ell_u + 2)\sigma, \sigma \in \mathbb{Z}_{\geq 0}\},$$
$$\bar{\mathcal{S}}_\alpha^y \doteq \{i \in \mathbb{N} : i = \alpha + 1 + (\ell_y + \ell_u + 2)\sigma, \sigma \in \mathbb{Z}_{\geq 0}\},$$
$$\bar{\mathcal{S}}_\beta^y \doteq \{i \in \mathbb{N} : i = \beta + \ell_y + 2 + (\ell_y + \ell_u + 2)\sigma, \sigma \in \mathbb{Z}_{\geq 0}\},$$

for $\alpha = 1, \ldots, \ell_y$ and $\beta = 1, \ldots, \ell_u$. It can be shown that the parameter $T$ in Lemma 8 is given by $T = T_{\text{S-RR}} \doteq \max\{2\ell_y + \ell_u + 2, 2\ell_u + \ell_y + 2\}$.

#### *5.3.2 Frequency Division Duplex Round Robin (FDD-RR)*

This scheduling protocol establishes a full-duplex communication link that uses two different frequency channels for measurements and actuation operations, see Table 3. For illustration purposes only, note that the superframe period in Table 3 is deliberately chosen to be different for the two channels.

Table 3
Superframe table for the FDD-RR protocol.

| | $t_1$ | $t_2$ | $\cdots$ | $t_{\ell_y}$ | $t_{\ell_y+1}$ |
|---|---|---|---|---|---|
| $\mathsf{CH}_1$ | $P \to D_1^y$ | $D_1^y \to D_2^y$ | $\cdots$ | $D_{\ell_y-1}^y \to D_{\ell_y}^y$ | $D_{\ell_y}^y \to C$ |
| $\mathsf{CH}_2$ | $C \to D_1^u$ | $D_1^u \to D_2^u$ | $\cdots$ | $D_{\ell_u}^u \to P$ | |

In this case, we have that $\delta_\alpha^y(i) \doteq 1 - \mathbb{1}_{\mathcal{D}_\alpha^y}(i)$, $\delta_\beta^u(i) \doteq 1 - \mathbb{1}_{\mathcal{D}_\beta^u}(i)$, $\gamma_\alpha^y(i) \doteq 1 - \mathbb{1}_{\bar{\mathcal{D}}_\alpha^y}(i)$, and $\gamma_\beta^u(i) \doteq 1 - \mathbb{1}_{\bar{\mathcal{D}}_\beta^u}(i)$, where

$$\mathcal{D}_\alpha^y \doteq \{i \in \mathbb{N} : i = \alpha + (\ell_y + 1)\sigma, \sigma \in \mathbb{Z}_{\geq 0}\},$$
$$\mathcal{D}_\beta^u \doteq \{i \in \mathbb{N} : i = \beta + (\ell_u + 1)\sigma, \sigma \in \mathbb{Z}_{\geq 0}\},$$
$$\bar{\mathcal{D}}_\alpha^y \doteq \{i \in \mathbb{N} : i = \alpha + 1 + (\ell_y + 1)\sigma, \sigma \in \mathbb{Z}_{\geq 0}\},$$
$$\bar{\mathcal{D}}_\beta^y \doteq \{i \in \mathbb{N} : i = \beta + 1 + (\ell_u + 1)\sigma, \sigma \in \mathbb{Z}_{\geq 0}\}$$

for $\alpha = 1, \ldots, \ell_y$ and $\beta = 1, \ldots, \ell_u$. For this case, the parameter $T$ in Lemma 8 is given by $T = T_{\text{FDD-RR}} \doteq \max\{2\ell_y + 1, 2\ell_u + 1\}$.

#### *5.3.3 Wave Round Robin (W-RR)*

This scheduling protocol schedules devices in an interleaved manner, see Table 4. That is, device one receives the measurement from the plant in the first timeslot, and at the same exact time (but in different frequency channels), device two transmits to device three and so on. Note that the number of channels used for the $y$-path (namely $M_y$), and the number of channels used for

Table 4
Superframe table for the W-RR protocol ($\ell_y$ even, $\ell_u$ odd).

| | $t_1$ | $t_2$ |
|---|---|---|
| $\mathsf{CH}_1$ | $P \to D_1^y$ | $D_1^y \to D_2^y$ |
| $\mathsf{CH}_2$ | $D_2^y \to D_3^y$ | $D_3^y \to D_4^y$ |
| $\vdots$ | $\vdots$ | $\vdots$ |
| $\mathsf{CH}_{M_y-1}$ | $D_{\ell_y-2}^y \to D_{\ell_y-1}^y$ | $D_{\ell_y-1}^y \to D_{\ell_y}^y$ |
| $\mathsf{CH}_{M_y}$ | $D_{\ell_y}^y \to C$ | |
| $\mathsf{CH}_{M_y+1}$ | $C \to D_1^u$ | $D_1^u \to D_2^u$ |
| $\mathsf{CH}_{M_y+2}$ | $D_2^u \to D_3^u$ | $D_3^u \to D_4^u$ |
| $\vdots$ | $\vdots$ | $\vdots$ |
| $\mathsf{CH}_{M_y+M_u-1}$ | $D_{\ell_u-3}^u \to D_{\ell_u-2}^u$ | $D_{\ell_u-2}^u \to D_{\ell_u-1}^u$ |
| $\mathsf{CH}_{M_y+M_u}$ | $D_{\ell_u-1}^u \to D_{\ell_u}^u$ | $D_{\ell_u}^u \to P$ |

the $u$-path (namely $M_u$) satisfy $M_y \doteq \frac{\ell_y+2-\theta_y}{2}$, $M_u \doteq \frac{\ell_u+2-\theta_u}{2}$, where $\theta_y, \theta_u \in \{0,1\}$. In particular, $\theta_y$ (resp. $\theta_u$) is 0 if $\ell_y$ (resp. $\ell_u$) is even, and 1 if $\ell_y$ (resp. $\ell_u$) is odd. Furthermore, it is important to note that in WH networks, the available number of channels is fixed (equal to 15). Therefore, $M_y$ and $M_u$ need to satisfy $M_y + M_u \leq 15$. However, this is not a problem because if there are too many field devices, the superframe period can always be increased to schedule the remaining devices that did not fit the 15 channels into another W-RR starting immediately after timeslot two.

For this example, $\delta^y_{1+2\alpha_1}(i) \doteq 1 - \mathbb{1}_{\mathcal{W}}(i)$, $\delta^y_{2+2\alpha_2}(i) \doteq \mathbb{1}_{\mathcal{W}}(i)$, $\delta^u_{1+2\beta_1}(i) \doteq 1 - \mathbb{1}_{\mathcal{W}}(i)$, $\delta^u_{2+2\beta_2}(i) \doteq \mathbb{1}_{\mathcal{W}}(i)$, $\gamma^y_\alpha(i) \doteq 1-\delta^y_\alpha(i)$, and $\gamma^u_\beta(i) \doteq 1-\delta^u_\beta(i)$, where $\mathcal{W} \doteq \{i \in \mathbb{N} : i = 1 + 2\sigma, \sigma \in \mathbb{Z}_{\geq 0}\}$, for $\alpha_1 = 0, 1, \ldots, \frac{\ell_y+\theta_y-2}{2}$, $\alpha_2 = 0, 1, \ldots, \frac{\ell_y-\theta_y-2}{2}$, $\beta_1 = 0, 1, \ldots, \frac{\ell_u+\theta_u-2}{2}$, $\beta_2 = 0, 1, \ldots, \frac{\ell_u-\theta_u-2}{2}$, $\alpha = 1, \ldots, \ell_y$, and $\beta = 1, \ldots, \ell_u$. For this case the parameter $T$ in Lemma 8 is given by $T = T_{\text{W-RR}} \doteq \max\{\ell_y + 2, \ell_u + 2\}$.

**Remark 10** *It can be seen that, exploiting multiple frequencies channels reduces the amount of timeslots required in the superframe (cf. Tables 2, 3 and 4). Specifically, it reduces the parameter $T$ related to the $PE_T$ property of the protocol. We note that, in particular, $T_{S\text{-}RR} > T_{FDD\text{-}RR} \geq T_{W\text{-}RR}$ for all $\ell_y, \ell_u \neq 0$. This will become important in Sections 6 and 8 when comparing the MATI bounds of these three protocols.* ■

## 6 $\mathcal{L}_p$ stability of WH–NCSs

In this section, we prove that $PE_T$ protocols lead to $\mathcal{L}_p$ stability of the WH–NCS. Inspired by the results in [24], we show that by exploiting the structure of our model, we can further improve the MATI bounds in [24]. Note that $g$ in (12) has a particular structure in which several rows are equal to zero. To better reveal this structure from our model (10), we re-arrange the error vector $\zeta = (\zeta^y, \zeta^u)$ in (9) via a change of coordinates. That is, we define $\boldsymbol{\zeta} \doteq \mathcal{T}\zeta$, where $\mathcal{T}$ is a matrix such that

$$\begin{aligned}\dot{\boldsymbol{\zeta}} &= \mathcal{T} g(x, \zeta, w) \doteq \boldsymbol{g}(x, \boldsymbol{\zeta}, w) \\ &= \begin{bmatrix} -\frac{\partial g_p}{\partial x_p} f_p(x_p, \mathbf{I}^{2\ell_u}_{n_u} \cdot \zeta^u + g_c(x_c), w) \\ -\frac{\partial g_c}{\partial x_c} f_c(x_c, \mathbf{I}^{2\ell_y}_{n_y} \cdot \zeta^y + g_p(x_p), w) \\ 0 \\ \vdots \\ 0 \end{bmatrix}\end{aligned} \tag{15}$$

Note that the first two components of $\dot{\boldsymbol{\zeta}}$ are non-zero while the rest are zero. This mathematical structure is key in the following stability results, and it comes directly from our modelling study in Section 4.

We impose the following assumption on the $\zeta$-subsystem.

**Assumption 11** *Let $L_{11} \in \mathcal{A}^{n_{\zeta^y_1}+n_{\zeta^u_1}}_{\geq 0}$ and $L_{12} \doteq L_{11}\, diag\{\mathbf{I}^{2\ell_y-1}_{n_y}, \mathbf{I}^{2\ell_u-1}_{n_u}\}$. There exists a matrix $A \in \mathcal{A}^{n_\zeta}_{\geq 0}$ of the form*

$$A = \begin{bmatrix} L_{11} & L_{12} \\ 0 & 0 \end{bmatrix}, \tag{16}$$

*and a continuous function $\tilde{y} : \mathbb{R}^{n_x} \times \mathbb{R}^{n_w} \to \mathbb{R}^{n_\zeta}_+$ such that the error dynamics* (10b) *satisfy*[1]

$$\dot{\bar{\boldsymbol{\zeta}}} = \bar{\boldsymbol{g}}(x, \zeta, w) \preceq A\bar{\boldsymbol{\zeta}} + \tilde{y}(x, w), \tag{17}$$

*for all $(x, \zeta, w) \in \mathbb{R}^{n_x} \times \mathbb{R}^{n_\zeta} \times \mathbb{R}^{n_w}$.* ■

Assumption 11 is the vector analogue of the dissipation type inequality imposed on the network-induced error system in [18], or many other works on non-linear NCSs [17, 19, 27]. This type of inequality essentially requires that the network-induced error exponentially grows during flows. Such a property is natural, as the $\boldsymbol{\zeta}$-system is typically unstable between two transmission instants.

Assumption 11 is also particularly inspired by (38) in [24]. However, in [24], the function $g$ does not have the structure in (15) that follows directly from our model. Note that $\bar{\boldsymbol{g}}$ has the form $(\bar{\boldsymbol{g}}_1, \bar{\boldsymbol{g}}_2, 0, \cdots, 0)$, and that $\boldsymbol{g}_1$ and $\boldsymbol{g}_2$ depend on sums of the components of $\boldsymbol{\zeta}$ (instead of the whole error as in [24]). Then, we can assume a linear bound on each component as in [24], i.e. we assume that there exist $L_1 \in \mathcal{A}^{n_y \times n_u}_{\geq 0}$, $L_2 \in \mathcal{A}^{n_u \times n_y}_{\geq 0}$ and functions $\tilde{y}_1 : \mathbb{R}^{n_x} \times \mathbb{R}^{n_w} \to \bar{\mathbb{R}}^{n_y}$ and $\tilde{y}_2 : \mathbb{R}^{n_x} \times \mathbb{R}^{n_w} \to \mathbb{R}^{n_y}$, such that $\bar{\boldsymbol{g}}_1(x, \mathbf{I}^{2\ell_u}_{n_u} \cdot \zeta^u, w) \leq L_1(\bar{\zeta}^u_1 + \cdots + \bar{\zeta}^u_{2\ell_u}) + \tilde{y}_1(x, w)$, $\bar{\boldsymbol{g}}_2(x, \mathbf{I}^{2\ell_y}_{n_y} \cdot \zeta^y, w) \leq L_2(\bar{\zeta}^y_1 + \cdots + \bar{\zeta}^y_{2\ell_y}) + \tilde{y}_2(x, w)$. Then, given the definition of $\boldsymbol{\zeta}$, we naturally get the bound in (17), i.e.

$$\bar{\boldsymbol{g}} \preceq \begin{bmatrix} 0 & L_1 & 0 & L_1\mathbf{I}^{2\ell_u-1}_{n_u} \\ L_2 & 0 & L_2\mathbf{I}^{2\ell_y-1}_{n_y} & 0 \\ 0 & 0 & 0 & 0 \\ \vdots & \vdots & \vdots & \vdots \\ 0 & 0 & 0 & 0 \end{bmatrix} \bar{\boldsymbol{\zeta}} + \begin{bmatrix} \tilde{y}_1(x, w) \\ \tilde{y}_2(x, w) \\ 0 \\ \vdots \\ 0 \end{bmatrix},$$

for $\star \in \{y, u\}$, and thus $L_{11}, L_{12}$ and $\tilde{y}(x, w)$ in Assumption 11 follow. We will show in Section 7 that the block structure of $A$ in (16) arises naturally in linear systems.

This next theorem states, in essence, that for sufficiently small MATI, the class of $PE_T$ protocols in Section 5.2 lead to the finite $\mathcal{L}_p$ stability of the $\zeta$-subsystem, which is key to prove Theorem 4 below. The proof can be found in the appendix.

[1] Recall that for any $x \in \mathbb{R}^n$, $\bar{x} \doteq (|x_1|, \ldots, |x_n|)^T$.

**Theorem 3** *Suppose that the scheduling protocol* (10d) *is persistently exciting in time $T$ and that Assumption 11 holds. Further suppose that MATI satisfies $\tau \in [\varepsilon, \tau^*)$, $\varepsilon \in (0, \tau^*)$ where $\tau^* = \ln\left(1 + 1/\sqrt{\varrho}\right)/(|L_{11}|T)$, and $\varrho \doteq \max\{2\ell_y, 2\ell_u\}$. Then, the system* (10b), (10d) *is $\mathcal{L}_p$ stable from $\tilde{y}$ to $\boldsymbol{\zeta}$ for $p \in [1, \infty]$ with gain*

$$\tilde{\gamma}(\tau) = \frac{T \exp(|A|(T+1)\tau)(\exp(|A|\tau) - 1)}{|A|\left(1 - \sqrt{\varrho}\left(\exp(|L_{11}|T\tau) - 1\right)\right)}. \tag{18}$$

■

The following theorem provides the closed-loop $\mathcal{L}_p$ stability result for the WH–NCS in (10), and is the main result of this section. It asserts that $PE_T$ protocols lead to $\mathcal{L}_p$ stability of the WH–NCS for sufficiently small MATI.

**Theorem 4** *Consider the WH–NCS* (10) *and suppose that*

*(1) The conditions of Theorem 3 hold with $\tilde{y} = G(x) + w$;*
*(2)* (10a) *is $\mathcal{L}_p$ stable from $(\boldsymbol{\zeta}, w)$ to $G(x)$ with gain $\gamma$ for some $p \in [1, \infty]$;*
*(3) MATI satisfies $\tau \in [\varepsilon, \tau^*)$, $\varepsilon \in (0, \tau^*)$, where $\tau^* = \ln(z)/(|A|T)$, $A$ comes from Assumption 11, and $z$ solves*

$$\gamma T z^{1+2/T} - \gamma T z^{1+1/T} + \sqrt{\varrho}|A| z^{|L_{11}|/|A|} - (1 + \sqrt{\varrho})\,|A| = 0. \tag{19}$$

*Then, the WH–NCS is $\mathcal{L}_p$ stable from $w$ to $(G(x), \boldsymbol{\zeta})$ with linear gain.*

**PROOF.** The proof follows from the fact that $\tilde{\gamma}(\tau)$ in (18) is differentiable and monotonically increasing in $\tau$ for $\tau \in [\varepsilon, \ln(1 + 1/\sqrt{\varrho})/|L_{11}|T]$ and thus, in view of the inverse function theorem [22], there exists a unique solution $\tau^*$ to $\tilde{\gamma}(\tau)\gamma = 1$. That is, $\gamma T \exp(|A|(T+1)\tau)(\exp(|A|\tau) - 1) - |A|\left(1 - \sqrt{\varrho}\left(\exp(|L_{11}|T\tau) - 1\right)\right) = 0$, for which we define $z \doteq \exp(|A|T\tau)$ and thus get (19). Then, by monotonicity of $\tilde{\gamma}(\tau)$, we have that $\tilde{\gamma}(\tau)\gamma < 1$ for any $\tau \in [\varepsilon, \tau^*)$. The proof is complete in light of the small-gain Theorem 1. ■

It is not immediately clear how the MATI bound $\tau^*$ behaves for different values of $T$. From Remark 10 we know that $T_{\text{S-RR}} > T_{\text{FDD-RR}} \geq T_{\text{W-RR}}$ for all $\ell_y, \ell_u \neq 0$. Intuition suggests that protocols exploiting multiple frequencies to schedule devices, i.e. smaller $T$, would lead to larger MATI bounds. In fact, if we take less time to get a packet from plant to controller (or vice-versa) then the inter-transmission bound may not need to be small in order to preserve stability. However, if we design a scheduling protocol in which the packet takes longer to reach the controller (e.g. S-RR), then faster transmission is required in order to preserve stability. Hence, we would expect that $\tau^*_{\text{S-RR}} \leq \tau^*_{\text{FDD-RR}} \leq \tau^*_{\text{W-RR}}$. In Section 8, we provide numerical examples in which this statement indeed holds.

In the proof of Theorem 4, the $\mathcal{L}_p$ stability property is obtained from an $\mathcal{L}_1$ bound, see (A.19). Such $\mathcal{L}_1$ bound is computed under the definition of $\|\cdot\|_{\mathcal{L}_p}$ in (1) with $\|\cdot\| \doteq |\cdot|$. However, using $\|\cdot\| \doteq \|\cdot\|_p$ in (1) to define $\|\cdot\|_{\mathcal{L}_p}$ (and thus $\|\cdot\|_{\mathcal{L}_1}$) will be particularly useful given the structure of $A$. In particular, we will see that this approach provides larger MATI bounds than the ones obtained in Theorem 4. To be precise and consistent with the above discussion, in Theorem 5 and Theorem 6, the definition of $\mathcal{L}_p$ stability is as per Definition 1 with $\|\cdot\|_{\mathcal{L}_p}$ as in (1), with $\|\cdot\| \doteq \|\cdot\|_p$.

**Theorem 5** *Suppose that the scheduling protocol* (10d) *is persistently exciting in time $T$ and that Assumption 11 holds. Further suppose that MATI satisfies $\tau \in [\varepsilon, \tau^*)$, $\varepsilon \in (0, \tau^*)$ where $\tau^* = \ln(2)/(\|L_{11}\|_1 T)$. Then, the NCS error subsystem* (10b)-(10d) *is $\mathcal{L}_p$ stable from $\tilde{y}$ to $\boldsymbol{\zeta}$ for $p \in [1, \infty]$ with gain*

$$\tilde{\gamma}(\tau) = \frac{T \exp(\|L_{11}\|_1(T+1)\tau)(\exp(\|L_{11}\|_1\tau) - 1)}{\|L_{11}\|_1(2 - \exp(\|L_{11}\|_1 T\tau))}.$$

**PROOF.** The proof follows along similar lines to the proof of Theorem 3. However, we use the definition of $\|\cdot\|_{\mathcal{L}_p}$ as in (1) with $\|\cdot\| \doteq \|\cdot\|_p$. Specifically, we use this definition in (A.19) when computing the $\mathcal{L}_1$ bound. Therefore, instead of having inequalities with Euclidean norm as in (A.18), we now bound $\|\bar{\boldsymbol{\zeta}}(\vartheta)\|_1$ so that we get $\|\bar{\boldsymbol{\zeta}}\|_{\mathcal{L}_1[t_k, t_{k+1}]}$ with the current definition. We point out here the important differences, in which the structure of $A$ plays a crucial role. The first significant difference appears when dealing with terms of the form (cf. (A.4))

$$\exp(AT\tau) - I = \begin{bmatrix} \exp(L_{11}T\tau) - I & 0 \\ 0 & 0 \end{bmatrix} \begin{bmatrix} I & \mathbf{I}_{y,u} \\ 0 & 0 \end{bmatrix},$$

where $\mathbf{I}_{y,u} \doteq \operatorname{diag}\{\mathbf{I}_{n_y}^{2\ell_y - 1}, \mathbf{I}_{n_u}^{2\ell_u - 1}\}$. By definition of the induced 1-norm of a matrix, definition of matrix exponential and triangle inequality, we have that

$$\begin{aligned} \left\| \exp(AT\tau) - I \right\|_1 &\leq \left\| \begin{bmatrix} \exp(L_{11}T\tau) - I & 0 \\ 0 & 0 \end{bmatrix} \right\|_1 \left\| \begin{bmatrix} I & \mathbf{I}_{y,u} \\ 0 & 0 \end{bmatrix} \right\|_1 \\ &= \left\| \exp(L_{11}T\tau) - I \right\|_1 \cdot 1 \\ &\leq \exp(\|L_{11}\|_1 T\tau) - 1. \end{aligned} \tag{20}$$

The other significant difference is that we can bound terms of the form $\exp(At)$, for any $t \geq 0$, as follows $\|\exp(At)\|_1 = \|\exp(At) - I + I\|_1 \leq \|\exp(At) - I\|_1 + \|I\|_1$. Now, we can use (20) in the last inequality to obtain $\|\exp(At)\|_1 \leq \exp(\|L_{11}\|_1 t)$. Consequently, the in-

duced 1-norm suits the structure of $A$ perfectly in the sense that we can now bound the exponential matrix $\exp(At)$ by a matrix that only depends on $L_{11}$. ■

**Theorem 6** *Consider the WH–NCS* (10) *and suppose that*

*(1) The conditions of Theorem 5 hold with $\tilde{y} = G(x) + w$;*
*(2)* (10a) *is $\mathcal{L}_p$ stable from $(\boldsymbol{\zeta}, w)$ to $G(x)$ with gain $\gamma$ for some $p \in [1, \infty]$;*
*(3) MATI satisfies $\tau \in [\varepsilon, \tau^*)$, $\varepsilon \in (0, \tau^*)$, where $\tau^* = \ln(z)/(\|L_{11}\|_1 T)$ and $z$ solves*

$$\gamma T z^{1+2/T} - \gamma T z^{1+1/T} + z\,\|L_{11}\|_1 - 2\|L_{11}\|_1 = 0.$$

*Then, the WH–NCS is $\mathcal{L}_p$ stable from $w$ to $(G(x), \boldsymbol{\zeta})$ with linear gain.* ■

## 7 Case study: The linear case

Consider the WH–NCS of Fig. 4 where the plant and controller have the following linear state-space form

$$\begin{aligned} \dot{x}_p &= A_p x_p + B_p \hat{u}, \quad & \dot{x}_c &= A_c x_c + B_c \hat{y}, \\ y &= C_p x_p, & u &= C_c x_c. \end{aligned} \tag{21}$$

Recall the network-induced error in (9) and the augmented state $x = (x_p, x_c)$, then (10a)-(10b), together with the re-arranged error $\boldsymbol{\zeta}$, becomes

$$\dot{x} = A_{11} x + A_{12} \boldsymbol{\zeta} \tag{22a}$$
$$\dot{\boldsymbol{\zeta}} = A_{21} x + A_{22} \boldsymbol{\zeta}. \tag{22b}$$

where

$$A_{11} \doteq \begin{bmatrix} A_p & B_p C_c \\ B_c C_p & A_c \end{bmatrix},$$
$$A_{12} \doteq \begin{bmatrix} 0 & B_p & 0 & B_p \mathbf{I}_{n_y}^{2\ell_y - 1} \\ B_c & 0 & B_c \mathbf{I}_{n_u}^{2\ell_u - 1} & 0 \end{bmatrix},$$
$$A_{21} \doteq \begin{bmatrix} -[C_p \;\; 0] A_{11} \\ -[0 \;\; C_c] A_{11} \\ 0 \\ \vdots \\ 0 \end{bmatrix},$$
$$A_{22} \doteq \begin{bmatrix} 0 & -C_p B_p & 0 & -C_p B_p \mathbf{I}_{n_u}^{2\ell_u - 1} \\ -C_c B_c & 0 & -C_c B_c \mathbf{I}_{n_y}^{2\ell_y - 1} & 0 \\ 0 & 0 & 0 & 0 \\ \vdots & \vdots & \vdots & \vdots \\ 0 & 0 & 0 & 0 \end{bmatrix}.$$

With the above, we can state the following immediate result.

**Proposition 1** *Consider the linear system* (22)*. Then, Assumption 11 is satisfied with $A = \overline{A}_{22}$, and $\tilde{y}(x) \doteq \overline{A_{21}} x$, for any $x \in \mathbb{R}^{n_x}$, and thus Theorems 4 and 6 can be directly invoked to compute the MATI bound that ensures $\mathcal{L}_p$ stability of the linear system* (22)*.* ■

Note that Assumption 11 is naturally satisfied in linear WH–NCSs, given the structure of the WH network.

## 8 Numerical examples

### 8.1 MATI Computation

In this section, we numerically compare our MATI bounds to the bounds in [17, 24] on an example. We restrict the discussion of this section to linear time-invariant systems in the absence of exogenous disturbances, and we thus verify UGES via Theorem 2.

Table 5
MATI bounds achieving UGES for the linear example in Section 8.1, when the three $PE_T$ scheduling protocols of Section 5.3 are implemented. ($\ell_y = 2, \ell_u = 1$.)

| | S-RR | FDD-RR | W-RR |
|---|---|---|---|
| $\tau^*_{[17]}$ in [ms] | $5.11 \cdot 10^{-5}$ | $4.18 \cdot 10^{-3}$ | $3.86 \cdot 10^{-2}$ |
| $\tau^*_{[24]}$ in [ms] | 13.28 | 18.37 | 22.72 |
| $\tau^*_{\text{thm.4}}$ in [ms] | 13.53 | 18.69 | 23.1 |
| $\tau^*_{\text{thm.6}}$ in [ms] | 17.54 | 24.31 | 30.11 |
| $\tau^*_{\text{thm.4}}$ vs. $\tau^*_{[17]}$ | $2.65 \cdot 10^7\%$ | $4.47 \cdot 10^5\%$ | $5.97 \cdot 10^4\%$ |
| $\tau^*_{\text{thm.4}}$ vs. $\tau^*_{[24]}$ | 1.82% | 1.75% | 1.69% |
| $\tau^*_{\text{thm.6}}$ vs. $\tau^*_{[17]}$ | $3.43 \cdot 10^7\%$ | $5.81 \cdot 10^5\%$ | $7.79 \cdot 10^4\%$ |
| $\tau^*_{\text{thm.6}}$ vs. $\tau^*_{[24]}$ | 32% | 32.3% | 32.55% |

Consider the linear WH–NCS in (22) with $A_p = 0.5, B_p = 1.1, C_p = 1, D_p = 0$, $A_c = -2, B_c = -1, C_c = 1.5, D_c = 0$, and $\ell_y = 2, \ell_u = 1$. In this case,

$$A = \left[\begin{array}{cc|cccc} 0 & 1.1 & 0 & 0 & 0 & 1.1 \\ 1.5 & 0 & 1.5 & 1.5 & 1.5 & 0 \\ \hline 0 & 0 & 0 & 0 & 0 & 0 \\ 0 & 0 & 0 & 0 & 0 & 0 \\ 0 & 0 & 0 & 0 & 0 & 0 \\ 0 & 0 & 0 & 0 & 0 & 0 \end{array}\right],$$

and we note that $L_{11} = \begin{bmatrix} 0 & 1.1 \\ 1.5 & 0 \end{bmatrix}$, $|A| = 3$, and $|L_{11}| = \|L_{11}\|_1 = 1.5$. We implement the three scheduling protocols of Section 5.3, for which $T_{\text{S-RR}} = 7$, $T_{\text{FDD-RR}} = 5$ and $T_{\text{W-RR}} = 4$. We can compute the $\mathcal{L}_2$ gain from $\boldsymbol{\zeta}$ to $\tilde{y} = \overline{A_{21}} x$ using MATLAB and have $\gamma = 5.19$. With the above, Table 5 is constructed by using Theorems 4 and 6 to compute the MATI bounds $\tau^*_{\text{thm.4}}$ and $\tau^*_{\text{thm.6}}$ (both theorems can be directly invoked given Proposition 1). The bound $\tau^*_{[17]}$ is computed by using our previous work [17]. Then, $\tau^*_{[24]}$ is obtained by using the $PE_T$

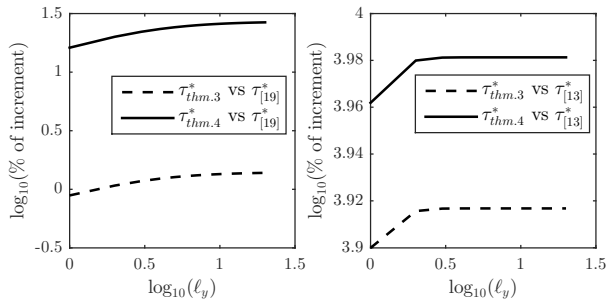


Fig. 5. Linear example: Percentage of improvement between $\tau^*_{\text{thm.4}}, \tau^*_{\text{thm.6}}$ and $\tau^*_{[24]}$ (left), and between $\tau^*_{\text{thm.4}}, \tau^*_{\text{thm.6}}$ and $\tau^*_{[17]}$ (right). ($\ell_y \in [1, 20]$ and W-RR.)

framework in [24], which does not exploit the structure of $A$. Next, we obtain the bounds $\tau^*_{\text{thm.3}}$ and $\tau^*_{\text{thm.4}}$, in view of Theorems 4 and 6. Note that we can use the same $\mathcal{L}_2$ gain $\gamma$ in both Theorems 4 and 6 given that $\|\cdot\|_{\mathcal{L}_p}$ in (1) with $\|\cdot\| \doteq |\cdot|$, for $p = 2$, coincides with $\|\cdot\|_{\mathcal{L}_p}$ when using $\|\cdot\| \doteq \|\cdot\|_p$. In order to have a clear comparison, we have also included, in the last four rows, the *percentage of improvement* between our proposed bounds $\tau^*_{\text{thm.4}}, \tau^*_{\text{thm.6}}$ and previous literature $\tau^*_{[17]}, \tau^*_{[24]}$. (We define the percentage of improvement between $\tau_A > 0$ and $\tau_B > 0$, where $\tau_A \geq \tau_B$, as $100 \times (\tau_A - \tau_B)/\tau_B$.)

We make the following comments:

(1) We can see that implementing a W-RR protocol results in larger MATI bounds in comparison to S-RR and FDD-RR. This is consistent with intuition.
(2) Our MATI bounds $\tau^*_{\text{thm.4}}$ and $\tau^*_{\text{thm.6}}$ are both larger than the bounds in previous works [17] and [24], given we exploit the mathematical structure of our WH–NCS model. In fact, the bound $\tau^*_{[17]}$ is quite conservative in the context of WH.
(3) The bound $\tau^*_{[17]} = 3.86 \cdot 10^{-2}[ms]$ (W-RR column) that preserves UGES is equivalent to a network throughput of 26.32 Mbps (WH has a maximum packet length of 127 bytes). However, the maximum data rate allowed in WH networks is 250 kbps, meaning that the bounds in [17] are quite conservative. Our current bounds $\tau^*_{\text{thm.3}} = 23.1[ms]$ and $\tau^*_{\text{thm.4}} = 30.11[ms]$, are equivalent to 43.98 kpbs and 33.74 kbps, respectively. These are actually achievable on current WH networks.
(4) When using Theorem 4, the corresponding bounds are larger by around 1.7%. This is a modest improvement but still tighter than [24]. Theorem 6 provides MATI bounds around 33% better. In addition, Figure 5 shows that the percentage of improvement between our bounds and [17,24] increases with the number of field devices.

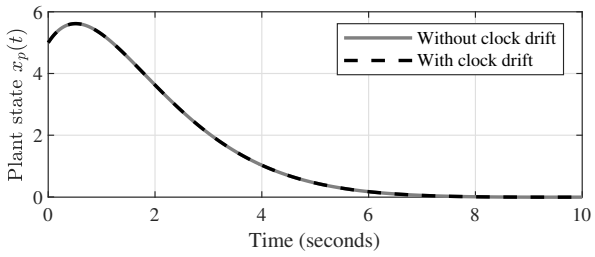


Fig. 6. Stabilisation of the plant (21) when the controller is implemented over a WH network via the TrueTime simulator without clock drift (solid line) and with clock drift (dashed line).

### *8.2* TrueTime *simulation of the WH–NCS*

We now present a simulation in TrueTime, which is a Simulink-based simulator for real-time control systems, including controller task execution, real-time kernels, network transmissions and continuous plant dynamics [12]. Consider the same linear plant and controller in Section 8.1. We have implemented the FDD-RR protocol from Section 5.3.2, in which the sensor measurements are sent in a RR fashion via channel one, and the control signal is sent via channel two. In the $y$-path we one sensor and one router (i.e. $\ell_y = 2$), and in the $u$-path we have one actuator (i.e. $\ell_u = 1$). All the communications are done through a WH network under TDMA communications. The controller and every field device are simulated with TrueTime kernel blocks, which are responsible for control logic, network data acquisition, data processing and calculations. The TrueTime network block simulates the transfer of packets in a real network, in this case, a WH network.

In Figure 6, we can see that the controller can successfully stabilise the plant from an initial condition of $x_p(0) = 5$ when implemented over a WH network. In the same figure, we supposed that the actuator is subject to clock drift with respect to the field devices in the $y$-path, which can be explicitly added in the TrueTime kernel block. That is, we are perturbing Assumption 4(a), and thus transmissions in channel one might not happen at the same time as transmissions in channel two. The usual clock drift in digital devices is around 10 parts-per-million (ppm), and we have used this value in the simulation. We can see from Figure 6 that the controller is still capable of stabilising the plant even when field devices are subject to clock drift.

## 9 Conclusions

This paper studied general non-linear control systems with disturbances that are implemented over WH networks. We first provided a hybrid model of WH–NCSs, which captures most functionalities of the network. Such model is then used to study $\mathcal{L}_p$ stability of WH–NCSs. In particular, we showed that, for high enough transmission

rates, a scheduling protocol that regularly schedules to transmit every field device within a fixed period of time ought to preserve $\mathcal{L}_p$ stability of the network-free system. We thus provided guidelines to design scheduling protocols, implementable in WH under TDMA communications, such that this property is indeed satisfied. Quantitatively, this paper provided sharp MATI bounds, significantly improving upon bounds provided in [17] and [24]. This improvement relies exclusively on exploiting the mathematical structure of our model. Future work will focus on studying the tracking problem, and also on obtaining results for more general network topologies.

## A Appendix

### *A.1 Technical lemmas*

In order to prove the main results of this paper, we first need the following lemmas.

**Lemma 12** *Let $A, B \in \mathcal{A}^n_{\geq 0}$, and suppose $A \preceq B$. Then: $\forall x \in \mathbb{R}^n_{\geq 0}, Ax \preceq Bx$; $\forall C \in \mathcal{A}^n_{\geq 0}, AC \preceq BC$; and $\forall C \in \mathcal{A}^n_{\geq 0}, CA \preceq CB$.* ■

**Lemma 13 (cf. [24, 25])** *Let $v \in \mathbb{R}^n$ and consider $Dv(t) \preceq Av(t) + d(t)$ with $v(t_0) = v_0$, for all $t \in I \subset \mathbb{R}$, where $Dv(t)$ denotes the left-handed derivative of $v(t)$, $A \in \mathcal{A}^n_{\geq 0}$ and $d(t) : I \to \mathbb{R}^n$ is continuous. Then, $v(t)$ is bounded by $v(t) \preceq \exp(A(t-t_0))v_0 + \int_{t_0}^{t} \exp(A(t-s))d(s)\,ds$, for all $t \in I$.* ■

**Lemma 14** *Suppose that $A \in \mathcal{A}^n_{\geq 0}$ has the block structure in (16), and $\{Q_i\}_{i\in\mathbb{N}} \in \mathfrak{S}_n(T)$ are arbitrary. Then $\left|\left(\prod_{i=n}^{n+T-1} Q_i \exp(A\tau)\right)\right| \leq \lambda < 1$, for all $n \in \mathbb{N}$, and all $\tau \in [0, \tau^*)$, where $\tau^* = \ln\left(1 + 1/\sqrt{\varrho}\right)/(|L_{11}|T)$, and $\lambda \doteq (\exp(|L_{11}|T\tau) - 1)\sqrt{\varrho}$, and $\varrho \doteq \max\{2\ell_y, 2\ell_u\}$.*

**PROOF.** Fix $n \in \mathbb{N}$ and $\tau \in \mathbb{R}$. By following the induction procedure in the proof of Lemma 7.1 in [24], together with properties (2) and (3) of Lemma 12, we get

$$\left(\prod_{i=n}^{n+T-1} Q_i \exp(A\tau)\right) \preceq \left(\prod_{i=n}^{n+T-1} Q_i\right) + \exp(AT\tau) - I.$$

Then, given that $\{Q_i\}_{i\in\mathbb{N}} \in \mathfrak{S}_n(T)$,

$$\left|\left(\prod_{i=n}^{n+T-1} Q_i \exp(A\tau)\right)\right| \leq |\exp(AT\tau) - I|. \quad (A.1)$$

We now exploit the structure of $A$. Note that since $A$ has the block structure in (16), we have that, by definition of the matrix exponential

$$\exp(AT\tau) - I = \begin{bmatrix} L_{11} & L_{12} \\ 0 & 0 \end{bmatrix} T\tau + \frac{1}{2!}\begin{bmatrix} L_{11}^2 & L_{11}L_{12} \\ 0 & 0 \end{bmatrix}(T\tau)^2 + \cdots \quad (A.2)$$

Now, note that by definition of $L_{12}$ in Assumption 11, we have that

$$L_{12}T\tau + \frac{1}{2!}L_{11}L_{12}(T\tau)^2 + \cdots = (\exp(L_{11}T\tau) - I)\mathbf{I}_{y,u}. \quad (A.3)$$

Given (A.2) and (A.3), we have that

$$\exp(AT\tau) - I = \begin{bmatrix} \exp(L_{11}T\tau) - I & 0 \\ 0 & 0 \end{bmatrix}\begin{bmatrix} I & \mathbf{I}_{y,u} \\ 0 & 0 \end{bmatrix}. \quad (A.4)$$

Therefore, the induced 2-norm of $\exp(AT\tau) - I$ can be bounded as follows

$$|\exp(AT\tau) - I| \leq \left|\begin{bmatrix} \exp(L_{11}T\tau) - I & 0 \\ 0 & 0 \end{bmatrix}\right| \left|\begin{bmatrix} I & \mathbf{I}_{y,u} \\ 0 & 0 \end{bmatrix}\right| = |\exp(L_{11}T\tau) - I|\sqrt{\max\{\varrho\}}, \quad (A.5)$$

where the last equality follows from the definition of 2-norm and $\mathbf{I}_{y,u}$. Then,

$$|\exp(L_{11}T\tau) - I| \leq |L_{11}|T\tau + \frac{1}{2!}|L_{11}|^2(T\tau)^2 + \cdots = \exp(|L_{11}|T\tau) - 1. \quad (A.6)$$

Putting together (A.1), (A.5) and (A.6) we can conclude

$$\left|\left(\prod_{i=n}^{n+T-1} Q_i \exp(A\tau)\right)\right| \leq |\exp(AT\tau) - I| \leq (\exp(|L_{11}|T\tau) - 1)\sqrt{\varrho}. \quad (A.7)$$

It is clear now that we need to choose $\tau$ such that (A.7) is less than one. We thus let $(\exp(|L_{11}|T\tau^*) - 1)\sqrt{\varrho} = 1$, and get $\tau^* = \ln\left(1 + 1/\sqrt{\varrho}\right)/(|L_{11}|T)$. By monotonicity of $(\exp(|L_{11}|T\tau) - 1)\sqrt{\varrho}$ in $\tau$, (A.7) is less than one for all $[0, \tau^*)$, completing the proof. ■

### *A.2 Proof of Lemma 8*

Consider a scheduling protocol that satisfies Assumption 7. Then, the corresponding protocol equation is given by (10d) with $\mathcal{H}(i)$ satisfying (13). Now, consider the following auxiliary discrete-time system

$$\zeta(k+1) = \mathcal{H}(k)\zeta(k), \quad (A.8)$$

initialized at time $i$ with initial condition $\zeta(i) = \zeta$. The solution of this system at time $k$, starting at time $i$ and

initial condition $\zeta$ is denoted by $\phi(k,i,\zeta)$, and it is given by $\phi(k,i,\zeta) = \big(\prod_{j=i}^{k-1}\mathcal{H}(j)\big)\zeta$. Now, recall from Section 5.1 that $\mathcal{H}(i)$ depends on $\gamma_\alpha^y(i), \gamma_\beta^u(i), \delta_\alpha^y(i), \delta_\beta^u(i)$ which take values in $\{0,1\}$, and these are related to the components of $\zeta$ being reset to zero whenever transmissions take place. Therefore, if every field device transmits within $T$ units of time, it means that every component of the error would have been reset to zero in that period. Therefore, there exists $T \in \mathbb{N}$ such that the solution of the discrete-time system (A.8) satisfies $\phi(T+i,i,\zeta) = 0$ for all $i \in \mathbb{N}$ and $\zeta \in \mathbb{R}^{n_\zeta}$. That is, $\big(\prod_{j=i}^{T+i-1}\mathcal{H}(j)\big)\zeta = 0$, for all $i \in \mathbb{N}$ and $\zeta \in \mathbb{R}^{n_\zeta}$. Because the latter holds for every $\zeta \in \mathbb{R}^{n_\zeta}$, we conclude that $\mathcal{H}$ satisfies (14) for some $T \in \mathbb{N}$, completing the proof. ■

### *A.3 Proof of Theorem 3*

Define $Q_i \doteq \mathcal{H}(i)$ for each $i \in \mathbb{N}$, and assume the system is initialised at time $t_s$, $t_s \in [0,t_0]$, $t_0 - t_s < \tau$. Given that the protocol is $PE_T$, then $\{Q_i\}_{i\in\mathbb{N}} \in \mathfrak{S}_{n_\zeta}(T)$. For simplicity, we write $\tilde{y}(s)$ instead of $\tilde{y}(x(s),w(s))$. By hypothesis, we have that $\bar{\boldsymbol{g}}(x,\boldsymbol{\zeta},w) = \dot{\bar{\boldsymbol{\zeta}}} \preceq A\bar{\boldsymbol{\zeta}} + \tilde{y}(t)$, for almost all $t \in [t_i, t_{i+1}]$. The $\iota$-th component of $\dot{\bar{\boldsymbol{\zeta}}}$, $\iota \in \{1,\dots,2\ell_y + 2\ell_u\}$, is given by

$$\begin{aligned}\left|\frac{d}{dt}\boldsymbol{\zeta}_\iota(t)\right| &= \left|\lim_{h\to 0,h<0}\frac{\boldsymbol{\zeta}_\iota(t+h)-\boldsymbol{\zeta}_\iota(t)}{h}\right| \\ &\geq \lim_{h\to 0,h<0}\frac{|\boldsymbol{\zeta}_\iota(t+h)|-|\boldsymbol{\zeta}_\iota(t)|}{h} = D\bar{\boldsymbol{\zeta}}_\iota(t),\end{aligned}$$

hence $D\bar{\boldsymbol{\zeta}} \preceq A\bar{\boldsymbol{\zeta}} + \tilde{y}(t)$. We now apply Lemma 13 to this equation with initial condition $\bar{\boldsymbol{\zeta}}(t_{i-1}^+)$, together with the protocol equation (10d), to get

$$\begin{aligned}\bar{\boldsymbol{\zeta}}(t_i^+) \preceq\ & Q_i \exp(A(t_i - t_{i-1}))\bar{\boldsymbol{\zeta}}(t_{i-1}^+) \\ &+ Q_i\int_{t_{i-1}}^{t_i}\exp(A(t_i-s))\tilde{y}(s)ds. \quad \text{(A.9)}\end{aligned}$$

Define $R_i \doteq Q_i\exp(A\tau)$. By iterating the linear recurrence (A.9) from the initial condition $\bar{\boldsymbol{\zeta}}(t_s)$, and using Corollary 1, we get the following bound for all $k \in \mathbb{Z}_{\geq 0}$

$$\begin{aligned}\bar{\boldsymbol{\zeta}}(t_k^+) \preceq\ & \left(\prod_{i=0}^{k}R_i\right)\bar{\boldsymbol{\zeta}}(t_s) + \sum_{i=0}^{k}\left(\prod_{n=i}^{k}R_n\right) \\ &\times \exp(-A\tau)\int_{t_{i-1}}^{t_i}\exp(A(t_i-s))\tilde{y}(s)ds. \quad \text{(A.10)}\end{aligned}$$

Fix $\tau \in (0,\tau^*)$, where $\tau^*$ comes from Lemma 14. We first set the disturbance term $\tilde{y} = 0$ and we focus in the contribution of the initial condition $\bar{\boldsymbol{\zeta}}(t_s)$. Then, by using Lemma 14, we have that, for all $m \in \mathbb{N}$

$$|\bar{\boldsymbol{\zeta}}(t_{mT-1}^+)| \leq \left|\prod_{i=0}^{mT-1}R_i\right||\bar{\boldsymbol{\zeta}}(t_s)| \leq \lambda^m|\bar{\boldsymbol{\zeta}}(t_s)|. \quad \text{(A.11)}$$

From $D\bar{\boldsymbol{\zeta}} \preceq A\bar{\boldsymbol{\zeta}} + \tilde{y}(t)$ with $\tilde{y} = 0$, we have that $\bar{\boldsymbol{\zeta}}(s) \preceq \exp(A(s-s_0))\bar{\boldsymbol{\zeta}}(s_0)$ (cf. Lemma 13), for every $\bar{\boldsymbol{\zeta}}(s_0) \in \mathbb{R}^{n_\zeta}$. From the latter, and by using $\bar{\boldsymbol{\zeta}}(s_0) = \bar{\boldsymbol{\zeta}}(t_{mT-1}^+)$ and its bound in (A.11), we have that

$$|\bar{\boldsymbol{\zeta}}(\theta)| \leq \exp(|A|(\theta - t_{mT-1}))\lambda^m|\bar{\boldsymbol{\zeta}}(t_s)|, \quad \text{(A.12)}$$

for all $m \in \mathbb{N}$ and $\theta \in (t_{mT-1}, t_{(m+1)T-1})$. Raising (A.12) to the $p$-th power and integrating over $[t_{mT-1}, t_{(m+1)T-1}]$, we get

$$\big\|\bar{\boldsymbol{\zeta}}\big\|^p_{\mathcal{L}_p[t_{mT-1},t_{(m+1)T-1}]} \leq \frac{\lambda^{mp}}{p|A|}(\exp(|A|pT\tau)-1)|\bar{\boldsymbol{\zeta}}(t_s)|^p, \quad \text{(A.13)}$$

for all $m \in \mathbb{N}$ and all $p \in [1,\infty)$. Now, we need to compute a similar bound in the interval $[t_s, t_{T-1}]$. Proceeding as above, we have that

$$\big\|\bar{\boldsymbol{\zeta}}\big\|^p_{\mathcal{L}_p[t_s,t_{T-1}]} \leq \frac{1}{p|A|}(\exp(|A|pT\tau)-1)|\bar{\boldsymbol{\zeta}}(t_s)|^p, \quad \text{(A.14)}$$

for all $p \in [1,\infty)$. Therefore, by summing (A.14) and (A.13) with $m \to \infty$, and taking the $p$-th root, we have that, for all $t \geq t_s$

$$\begin{aligned}\big\|\bar{\boldsymbol{\zeta}}\big\|_{\mathcal{L}_p[t_s,t]} &\leq \sum_{i=0}^{\infty}\lambda^i\left(\frac{\exp(|A|pT\tau)-1}{p|A|}\right)^{1/p}|\bar{\boldsymbol{\zeta}}(t_s)| \\ &\leq \frac{1}{1-\lambda}\left(\frac{\exp(|A|pT\tau)-1}{p|A|}\right)^{1/p}|\bar{\boldsymbol{\zeta}}(t_s)|, \quad \text{(A.15)}\end{aligned}$$

where the last inequality follows from $\lambda < 1$ given Lemma 14. For $p = \infty$ we get the $\mathcal{L}_\infty$ bound by taking $\lim_{p\to\infty}\big\|\bar{\boldsymbol{\zeta}}\big\|_{\mathcal{L}_p[t_s,t]}$ in (A.15), that is,

$$\big\|\bar{\boldsymbol{\zeta}}\big\|_{\mathcal{L}_\infty} \leq \frac{1}{1-\lambda}\exp(|A|T\tau)|\bar{\boldsymbol{\zeta}}(t_s)|. \quad \text{(A.16)}$$

We now focus on bounding the contribution from the disturbance term in (A.10), obtained by setting $\bar{\boldsymbol{\zeta}}(t_s) = 0$. We get

$$\begin{aligned}\bar{\boldsymbol{\zeta}}(t_k^+) \preceq\ & \sum_{i=0}^{k}\left(\prod_{n=i}^{k}R_n\right)\exp(-A\tau) \\ &\times\int_{t_{i-1}}^{t_i}\exp(A(t_i-s))\tilde{y}(s)ds. \quad \text{(A.17)}\end{aligned}$$

Again, applying Lemma 13 to $D\bar{\boldsymbol{\zeta}} \preceq A\bar{\boldsymbol{\zeta}} + \tilde{y}(t)$ with initial condition (A.17), we get, for $\vartheta \in [t_k, t_{k+1}]$

$$\begin{aligned}\bar{\boldsymbol{\zeta}}(\vartheta) \preceq \exp(A(\vartheta - t_k)) \sum_{i=0}^{k} \left( \prod_{n=i}^{k} R_n \right) \\ \times \exp(-A\tau) \int_{t_{i-1}}^{t_i} \exp(A(t_i - s)) \tilde{y}(s) ds \\ + \int_{t_k}^{\vartheta} \exp(A(\vartheta - s)) \tilde{y}(s) ds.\end{aligned}$$

We now use the same division algorithm used in [24, Theorem 5.1] to show that

$$\left| \prod_{n=i}^{k} R_n \right| \leq \lambda^{\lfloor (k+1-i)/T \rfloor} \exp(|A|(T-1)\tau).$$

With the above we can get the following bound for all $\vartheta \in [t_k, t_{k+1}]$

$$\begin{aligned}|\bar{\boldsymbol{\zeta}}(\vartheta)| \leq \exp(|A|(\vartheta - t_k)) \exp(|A|T\tau) \sum_{i=0}^{k} \lambda^{\lfloor (k+1-i)/T \rfloor} \\ \times \int_{t_{i-1}}^{t_i} \exp(|A|(t_i - s)) |\tilde{y}(s)| ds \\ + \int_{t_k}^{\vartheta} \exp(|A|(\vartheta - s)) |\tilde{y}(s)| ds. \quad \text{(A.18)}\end{aligned}$$

In order to compute the $\mathcal{L}_p$ bound in this case, we will start by finding an $\mathcal{L}_1$ estimate. Define $\varphi(s) \doteq \exp(|A|s)$. We integrate (A.18) and use Young's inequality [9] to get

$$\begin{aligned}\left\| \bar{\boldsymbol{\zeta}} \right\|_{\mathcal{L}_1[t_k, t_{k+1}]} \leq \|\varphi\|_{\mathcal{L}_1[0,\tau]} \exp(|A|T\tau) \\ \times \sum_{i=0}^{k} \lambda^{\lfloor (k+1-i)/T \rfloor} \int_{t_{i-1}}^{t_i} \exp(|A|(t_i - s)) |\tilde{y}(s)| ds \\ + \|\varphi\|_{\mathcal{L}_1[0,\tau]} \|\tilde{y}\|_{\mathcal{L}_1[t_k, t_{k+1}]}.\end{aligned}$$

We can further bound the above as

$$\begin{aligned}\left\| \bar{\boldsymbol{\zeta}} \right\|_{\mathcal{L}_1[t_k, t_{k+1}]} \leq \|\varphi\|_{\mathcal{L}_1[0,\tau]} \exp(|A|(T+1)\tau) \\ \times \sum_{i=0}^{k} \lambda^{\lfloor (k+1-i)/T \rfloor} \|\tilde{y}\|_{\mathcal{L}_1[t_{i-1}, t_i]} \\ + \|\varphi\|_{\mathcal{L}_1[0,\tau]} \|\tilde{y}\|_{\mathcal{L}_1[t_k, t_{k+1}]} \\ \leq \|\varphi\|_{\mathcal{L}_1[0,\tau]} \exp(|A|(T+1)\tau) \\ \times \sum_{i=0}^{k+1} \lambda^{\lfloor (k+1-i)/T \rfloor} \|\tilde{y}\|_{\mathcal{L}_1[t_{i-1}, t_i]}. \quad \text{(A.19)}\end{aligned}$$

As in [24, Theorem 5.1], the bound on $\|\bar{\boldsymbol{\zeta}}\|_{\mathcal{L}_\infty[t_k, t_{k+1}]}$ is similar and omitted for brevity. Then, we can use the Riesz-Thorin interpolation theorem [23, p.52] to bound the $\mathcal{L}_p$ norm by the above $\mathcal{L}_1$ estimate. That is, summing (A.19) over the interval $[t_s, t_M]$, for all $M \geq 0$, we get

$$\begin{aligned}\left\| \bar{\boldsymbol{\zeta}} \right\|_{\mathcal{L}_p[t_s, t_M]} \leq \|\varphi\|_{\mathcal{L}_1[0,\tau]} \exp(|A|(T+1)\tau) \\ \times \sum_{k=-1}^{M-1} \sum_{i=0}^{k+1} \lambda^{\lfloor (k+1-i)/T \rfloor} \|\tilde{y}\|_{\mathcal{L}_p[t_{i-1}, t_i]},\end{aligned}$$

for $p \in [1, \infty]$. We now apply the Discrete Young's Inequality [24, Lemma 1.1], and take the limit as $M \to \infty$ in the above summation to get

$$\begin{aligned}\left\| \bar{\boldsymbol{\zeta}} \right\|_{\mathcal{L}_p[t_s, t_M]} \leq \|\varphi\|_{\mathcal{L}_1[0,\tau]} \exp(|A|(T+1)\tau) \\ \times \sum_{i=0}^{\infty} \lambda^{\lfloor i/T \rfloor} \sum_{i=0}^{\infty} \|\tilde{y}\|_{\mathcal{L}_p[t_{i-1}, t_i]} \\ = \|\varphi\|_{\mathcal{L}_1[0,\tau]} \exp(|A|(T+1)\tau) \\ \times \left( \frac{T}{1-\lambda} \right) \|\tilde{y}\|_{\mathcal{L}_p[t_s, t_M]} \\ = \frac{T \exp(|A|(T+1)\tau)(\exp(|A|\tau) - 1)}{|A| \left(1 + \sqrt{\varrho} - \sqrt{\varrho} \exp(|L_{11}|T\tau)\right)} \|\tilde{y}\|_{\mathcal{L}_p[t_s, t_M]}, \quad \text{(A.20)}\end{aligned}$$

where the last equality comes from the definition of $\varphi$, and the definition of $\lambda$ in Lemma 14. Note that either $\|\tilde{y}\|_{\mathcal{L}_p[t_s, t_M]} = 0$ or the ratio $\left\| \bar{\boldsymbol{\zeta}} \right\|_{\mathcal{L}_p[t_s, t_M]} / \|\tilde{y}\|_{\mathcal{L}_p[t_s, t_M]}$ is bounded by an expression that is independent of $M$, hence, (A.20) remains true with $t$ in lieu of $t_M$ for any $t \geq t_s$. To finish the proof, we sum both (A.15) and (A.20), to get

$$\begin{aligned}\left\| \bar{\boldsymbol{\zeta}} \right\|_{\mathcal{L}_p[t_s, t]} \leq \frac{1}{1 - \sqrt{\varrho} \left(\exp(|L_{11}|T\tau) - 1\right)} \\ \times \left( \frac{\exp(|A|pT\tau) - 1}{p|A|} \right)^{1/p} |\bar{\boldsymbol{\zeta}}(t_s)| \\ + \frac{T \exp(|A|(T+1)\tau)(\exp(|A|\tau) - 1)}{|A| \left(1 - \sqrt{\varrho} \left(\exp(|L_{11}|T\tau) - 1\right)\right)} \|\tilde{y}\|_{\mathcal{L}_p[t_s, t]}, \quad \text{(A.21)}\end{aligned}$$

for $p \in [1, \infty)$. The $\mathcal{L}_\infty$ bound is obtained by summing (A.16) and (A.20), that is

$$\begin{aligned}\left\| \bar{\boldsymbol{\zeta}} \right\|_{\mathcal{L}_\infty[t_s, t]} \leq \frac{\exp(|A|T\tau)}{1 - \sqrt{\varrho} \left(\exp(|L_{11}|T\tau) - 1\right)} |\bar{\boldsymbol{\zeta}}(t_s)| + \\ \frac{T \exp(|A|(T+1)\tau)(\exp(|A|\tau) - 1)}{|A| \left(1 - \sqrt{\varrho} \left(\exp(|L_{11}|T\tau) - 1\right)\right)} \|\tilde{y}\|_{\mathcal{L}_\infty[t_s, t]}. \quad \text{(A.22)}\end{aligned}$$

By using Definition 1 together with (A.21) and (A.22), we conclude that the system (10b), (10d) is $\mathcal{L}_p$ stable from $\tilde{y}$ to $\boldsymbol{\zeta}$ for $p \in [1, \infty]$ with gain $\tilde{\gamma}(\tau)$ as per (18). ■

## References


[1] HART Communication Protocol. `https://www.fieldcommgroup.org/technologies/hart`, 2007.

[2] A.W. Al-Dabbagh and T. Chen. A fixed structure topology for wireless networked control systems. In *Proceedings of the 55th Conference on Decision and Control*, pages 3450–3455, Las Vegas, U.S.A., 2016.

[3] R. Alur, A. d'Innocenzo, K.H. Johansson, G.J. Pappas, and G. Weiss. Compositional modeling and analysis of multi-hop control networks. *IEEE Transactions on Automatic control*, 56(10):2345–2357, 2011.

[4] M. De Biasi, C. Snickars, K. Landernas, and A.J. Isaksson. Simulation of process control with WirelessHART networks subject to clock drift. In *Proceedings of the 32nd Annual IEEE International Computer Software and Applications Conference*, 2008.

[5] D. Carnevale, A.R. Teel, and D. Nešić. A Lyapunov proof of an improved maximum allowable transfer interval for networked control systems. *IEEE Transactions on Automatic Control*, 52(5):892, 2007.

[6] D. Chen, M. Nixon, and A. Mok. *WirelessHART$^{TM}$: Real-Time Mesh Network for Industrial Automation*, pages 195–199. Springer US, Boston, MA, 2010.

[7] B. Demirel, Z. Zou, P. Soldati, and M. Johansson. Modular design of jointly optimal controllers and forwarding policies for wireless control. *IEEE Transactions on Automatic Control*, 59(12):3252–3265, 2014.

[8] P. Ferrari, A. Flammini, M. Rizzi, and E. Sisinni. Improving simulation of wireless networked control systems based on WirelessHART. *Computer Standards & Interfaces*, 35(6):605–615, 2013.

[9] D.H. Fremlin. *Measure theory*, volume 2. Torres Fremlin, 2001.

[10] S. Han, X. Zhu, K. Mok Aloysius, M. Nixon, T. Blevins, and D. Chen. Control over WirelessHART network. In *Proceedings of the 36th Annual Conference on IEEE Industrial Electronics Society*, 2010.

[11] W.P.M.H. Heemels and N. Van De Wouw. Stability and stabilization of networked control systems. In *Networked Control Systems*, pages 203–253. Springer, 2010.

[12] D. Henriksson, A. Cervin, and K.E. Årzén. Truetime: Simulation of control loops under shared computer resources. In *Proceedings of the 15th IFAC World Congress on Automatic Control*, 2002.

[13] J.P. Hespanha, P. Naghshtabrizi, and Y. Xu. A survey of recent results in networked control systems. *Proceedings of the IEEE*, 95(1):138–162, 2007.

[14] H.K. Khalil. *Nonlinear Systems*. Prentice-Hall, Upper Saddle River, NJ, second edition, 1996.

[15] A.I. Maass and D. Nešić. Stabilization of non-linear networked control systems closed over a lossy WirelessHART network. *IEEE Control Systems Letters*, 3(4):996–1001, 2019.

[16] A.I. Maass, D. Nešić, and P.M. Dower. A hybrid model of networked control systems implemented on WirelessHART networks under source routing configuration. In *Proceedings of the Australian Control Conference*, pages 60–65, Newcastle, Australia, 2016.

[17] A.I. Maass, D. Nešić, R. Postoyan, P.M. Dower, and V.S. Varma. Emulation-based stabilisation of networked control systems over WirelessHART. In *Proceedings of the 56th IEEE Conference on Decision and Control*, pages 6628–6633, Melbourne, Australia, 2017.

[18] D. Nešić and A.R. Teel. Input-output stability properties of networked control systems. *IEEE Transactions on Automatic Control*, 49(10):1650–1667, 2004.

[19] R. Postoyan, N. Van de Wouw, D. Nešić, and W.P.M.H. Heemels. Tracking control for nonlinear networked control systems. *IEEE Transactions on Automatic Control*, 59(6):1539–1554, 2014.

[20] A. Saifullah, D. Gunatilaka, P. Tiwari, M. Sha, C. Lu, B. Li, C. Wu, and Y. Chen. Schedulability analysis under graph routing in wirelesshart networks. In *Real-Time Systems Symposium, 2015 IEEE*, pages 165–174. IEEE, 2015.

[21] V.S. Soto, I. Muller, J.M. Winter, C.E. Pereira, and J.C. Netto. Control over wirelesshart network through a host application: A wirelesshart network control proposal. In *Computing Systems Engineering (SBESC), 2014 Brazilian Symposium on*, pages 91–96. IEEE, 2014.

[22] M. Spivak. *Calculus on manifolds: a modern approach to classical theorems of advanced calculus*. Westview Press, 1965.

[23] E.M. Stein and R. Shakarchi. *Functional analysis: introduction to further topics in analysis*, volume 4. Princeton University Press, 2011.

[24] M. Tabbara, D. Nešić, and A.R. Teel. Stability of wireless and wireline networked control systems. *IEEE Transactions on Automatic Control*, 52(9):1615–1630, 2007.

[25] P. Volkmann. Gewöhnliche differentialungleichungen mit quasimonoton wachsenden funktionen in topologischen vektorräumen. *Mathematische Zeitschrift*, 127(2):157–164, 1972.

[26] G.C. Walsh, O. Beldiman, and L.G. Bushnell. Asymptotic behavior of nonlinear networked control systems. *IEEE Transactions on Automatic Control*, 46(7):1093–1097, 2001.

[27] W. Wang, D. Nešić, and R. Postoyan. Emulation-based stabilization of networked control systems implemented on FlexRay. *Automatica*, 59:73–83, 2015.

[28] C. Wu, D. Gunatilaka, A. Saifullah, M. Sha, P.B. Tiwari, C. Lu, and Y. Chen. Maximizing network lifetime of wirelesshart networks under graph routing. In *Internet-of-Things Design and Implementation (IoTDI), 2016 IEEE First International Conference on*, pages 176–186. IEEE, 2016.

[29] H. Zhang, F. Österlind, P. Soldati, T. Voigt, and M. Johansson. Time-optimal convergecast with separated packet copying: Scheduling policies and performance. *IEEE Transactions on Vehicular Technology*, 64(2):793–803, 2015.

[30] H. Zhang, P. Soldati, and M. Johansson. Time- and channel-efficient link scheduling for convergecast in WirelessHART networks. In *Proceedings of the 13th IEEE International Conference on Communication Technology*, pages 99–103, Jinan, China, 2011.

[31] H. Zhang, P. Soldati, and M. Johansson. Performance bounds and latency-optimal scheduling for convergecast in WirelessHART networks. *IEEE Transactions on Wireless Communications*, 12(6):2688–2696, 2013.

[32] Z. Zou, B. Demirel, and M. Johansson. Minimum-energy packet forwarding policies for guaranteed LQG performance in wireless control systems. In *Proceedings of the 51st Conference on Decision and Control*, pages 3341–3346, Maui, Hawaii, 2012.